Smart Investment Framework for Energy Resilience: A Case Study of a Campus Microgrid Research Facility

SM Safayet Ullah[1], Samuel Yankson[1], Shayan Ebrahimi[1], Farzad Ferdowsi[1,*], and Terrence Chambers[2]

[1]Department of Electrical & Computer Engineering, University of Louisiana at Lafayette, Lafayette, 70503, LA, USA

[2]Department of Mechanical Engineering, University of Louisiana at Lafayette, Lafayette, 70503, LA, USA

[*]Corresponding author: ferdowsi@louisiana.edu

Abstract

Energy resilience is a vital consideration for ensuring the survivability of modern infrastructure systems. Achieving 100% resilience, however, is often impractical and economically burdensome. In this paper, we propose a smart investment framework that enables decision-makers to determine optimal investments in energy resilience based on available resources and desired levels of resilience. To illustrate the effectiveness of this framework, we present a case study of a campus microgrid research and testing facility. Using a real-time simulation approach conducted with Typhoon HIL, we evaluate the performance of the microgrid system over 24 hours following four historically significant hurricanes that have affected Louisiana in the past few years. The microgrid is designed to power local loads during outages, providing an effective solution for enhancing energy resilience. Real solar data collected from our 1.1 Megawatt (MW) solar facility on the University of Louisiana at Lafayette campus is integrated into the simulation, enabling a realistic evaluation of the system's performance under hurricane-induced disruptions. By employing the proposed smart investment framework, decision-makers can better identify and address resilience challenges. The framework facilitates informed investment decisions by considering available resources and aligning them with the desired level of resilience. This approach avoids over-investment in unnecessary redundancy while ensuring critical systems are adequately protected. Our research contributes to the field by demonstrating the practicality and benefits of a smart investment framework for energy resilience in a real-world scenario. The case study of the campus microgrid research

facility provides valuable insights for decision-makers in similar contexts, highlighting the potential of this framework to guide resilient energy infrastructure planning and investment strategies.

1. Introduction

Energy resilience assessment is becoming a critical part of contemporary power & energy systems at the design and operation levels, considering the increasing climate change impacts and natural disasters. Natural disasters can spread quickly, which affects the power grids heavily and creates a negative impact on society and the economy Bhusal et al., 2020; Dugan et al., 2021; Mukhopadhyay & Nateghi, 2017. These unwanted weather conditions are the main reasons for the major power outages, which cost billions of dollars as modern civilizations depend on the continuous utilization of power and energy. Different important sectors of the current civilization depend on the availability of electricity Dugan et al., 2021; Hossain et al., 2021. The expenditure of natural disasters is around \$25 to \$70 billion per year of the President. Council of Economic Advisers, 2013. According to the National Oceanic and Atmospheric Administration (NOAA), 20 natural disasters affected the USA in 2021, and each disaster's financial damage was over \$1 billion 'NOAA National Centers for Environmental Information (NCEI)', 2022. Due to natural disasters, power outages have happened more frequently in recent times, for instance, Hurricane Sandy, which occurred in 2012 and caused 8.5 million people to go out of power of the President. Council of Economic Advisers, 2013, the Hokkaido blackout of 2018 caused by an earthquake, blackouts in California in 2019, and the infamous Texas power outages in 2021 due to the winter storm Dugan et al., 2021; Kenward, Raja et al., 2014. In 2021, the National Oceanic and Atmospheric Administration (NOAA) named 2020 as the year of extremes. Within the past six years, five major hurricanes have hit Louisiana, including Nate (2017), Laura (2020), Delta (2020), Zeta (2020), and Ida (2021). These hurricanes left thousands of people out of power from a few hours to several days or even months Arora & Ceferino, 2023. In different sets of literature, increasing outages across the US are reported largely as a result of outdated infrastructure and grid consolidation. Despite this fact, replacing the grid anytime soon is highly unlikely, considering it would impose several trillion dollars on the US economy. Therefore, research around responsive and corrective approaches is of great importance to improve the grid's resilience.

Resilience is a fairly new concept in power systems. Although there are different definitions of resilience from various perspectives Arghandeh et al., 2016, a more general definition of resilience refers to the ability of a power system to withstand and absorb high-impact, low-probability (HILP) disturbances and quickly recover from those eventsAli et al., 2023. Withstanding severe disturbances (e.g., hurricanes) is mainly discussed under infrastructure resilience through hardening and related risk assessment activities Moglen et al., 2023; Schweikert & Deinert, 2021. On the other hand, operational resilience is linked to responsive and corrective control schemes as well as resource adequacy Abianeh & Ferdowsi, 2020; Ferdowsi et al., 2019. In order to improve resilience, it has to be quantified first. There are several methods reported in the literature for resilience quantification. This paper puts an emphasis on operational resilience rather than infrastructure. These two categories are well discussed in Hamidieh & Ghassemi, 2022.

Resilience metrics are required as the first step of the investigation to improve resilience. Several works have been done, and different resilience metrics and approaches are presented in the recent literature. Available resilience metrics can be classified into three main categories: attribute-based, performance-based, and general Daeli & Mohagheghi, 2023. Attribute-based resilience metrics mainly concentrate on the behavior of a system. Determining this type of metric requires reviewing the system's performance to measure the degree of the attributes held within it Vugrin et al., 2017. This type of resilience metric basically provides qualitative assessments. Performance-based metrics can be utilized to evaluate the efficiency of different types of reinforcement tactics installed in the system Vugrin et al., 2017. Performance-based metrics consist of two subcategories metrics: performance metrics and consequence metricsRaoufi et al., 2020; Vugrin et al., 2017. System performance metrics can model the behavior of the power system in accordance with the natural disasters, whereas consequence metrics concentrate on the impacts of power outages and can be quantified in the form of financial impacts, social impacts, and security impacts Raoufi et al., 2020; Vugrin et al., 2017. Several types of performance-based performance resilience metrics are available in the literatureRaoufi et al., 2020. Attribute-based metrics are comparatively easier to model as they depend on qualitative or semi-quantitative knowledge and analysis. However, this type of metric cannot analyze the benefits achieved from potential resilience enhancements and the effectiveness of investments. Hence, they are not as explanatory in comparison to performance-based metrics for grid resilience planning and investment strategies Vugrin et al., 2017. Performance-based metrics can be very complex and generally require a large amount of data to model as they model different stages of operation, disruption, and recovery Daeli & Mohagheghi, 2023. However, performance-based metrics are more dynamic than attribute-based metrics: not only can they be utilized to analyze the resilience of the system to previous events, but they can also simulate how the system will be affected by future events. General metrics can be utilized to portray different aspects of performance, functionality, impacts, etc. The Figure of Merit (FOM) curve is a common resilience assessment tool in dynamic systems, not necessarily power systems. FOM represents the functionality of a system in terms of the quantity/quality of services delivered by the system. The FOM has been used in different sets of literature for resilience analysis in different engineering systems such as transportation Janić, 2018 and energy Das et al., 2020. In some literature, FOM metric/curve is referred to as trapezoid Force et al., 2022 or triangle curve Panteli et al., 2017. The resilience curve and advanced trapezoidal resilience curve can be utilized as a general metric as they both can express different dimensions of performance or consequences Daeli & Mohagheghi, 2023. In Fig. 1, the resilience curve shows the changes in the resilience of the power network with respect to time. The quality indicator of the resilience curve can be based on attribute-based or performance-based metrics. Although it is very easy to interpret these types of curves, these curves are unable to collect all the different dynamic resilience dimensionsPanteli et al., 2017.

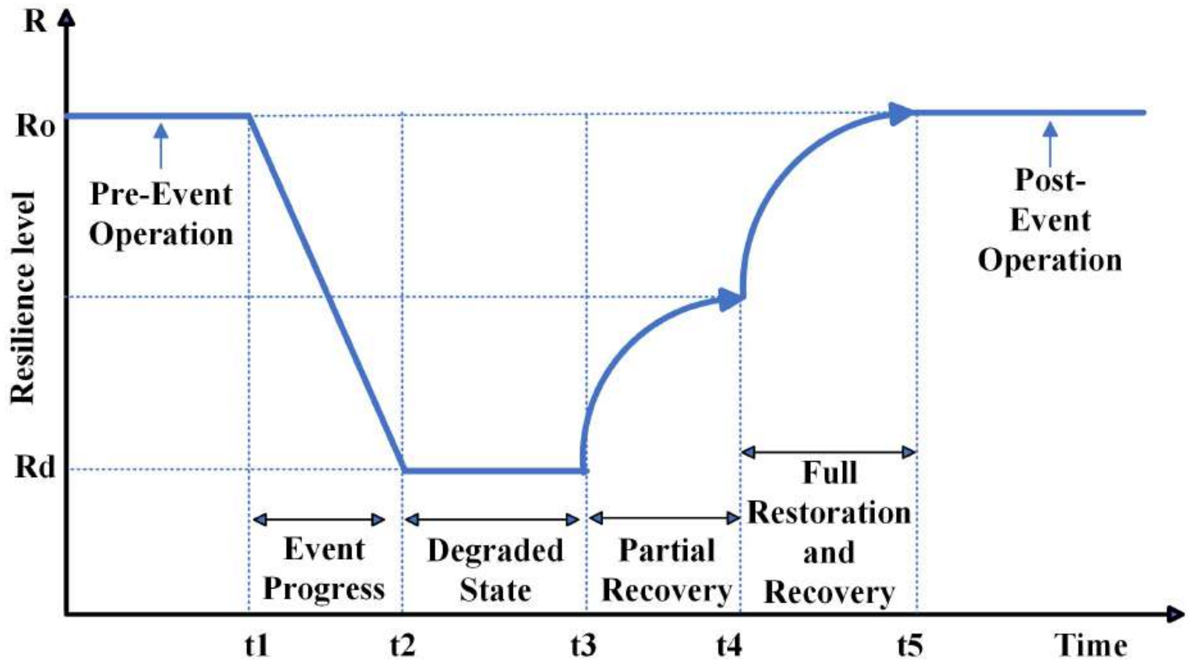

Figure 1: Traditional Resilience Curve Bie et al., 2017; Daeli & Mohagheghi, 2023; Lei et al., 2018; Mishra et al., 2020

While it is very important to measure the resilience of an existing system, it is also very important to investigate the enhancement of the resilience of the system as well as the necessary investment in comparison to the benefits and value it generates to the whole systemAnderson et al., 2020. It is neither practical nor economical to have an energy system that can fully withstand and absorb a wide range of disturbances with a very high level of robustness and continue its service with no interruption. Therefore, effective investment in the area of achievable resilience is of great importance in power systems. In order to achieve a more resilient power system, microgrids with the capability of operating in islanded mode are locally impactful if they can quickly respond to the loss of the main grid and feed the local loads. The extent to which a microgrid can contribute to serving the local loads after the main grid goes down depends on 1) the microgrid's resourcefulness and 2) the energy management strategy, assuming microgrid assets have survived the severe event. Microgrid is proposed in many academic studies and industry reports as a promising solution to expedite the restoration process Igder et al., 2022 and mitigate the duration/frequency of outages Khodayar et al., 2012 and/or impacts of outages Lin et al., 2022. Some of the commonly proposed improvement methods include prediction Mohammadian et al., 2021, load shedding Li et al., 2017; Sedzro et al., 2018, reconfiguration Choobineh & Mohagheghi, 2015; Ding et al., 2020, and mobile resources Lei et al., 2016. These improvement strategies are more tied to microgrid planning. From the operation's standpoint, resilience-oriented energy management techniques have been proposed in some research works recently Gholami et al., 2016; Liu et al., 2020. However, the proposed energy management techniques are more in the form of optimization-driven scheduling in microgrids. When it comes to energy resilience, planning and operation are complementary, which is not well discussed in the existing literature. Furthermore, energy planners and decision-makers need to have an insight into the cost of resilience so they can better invest to meet certain requirements and needs. The relationship between resilience improvement and necessary cost is not well investigated in the literature. In Benallal et al., 2023, Bayesian inference-based energy management was proposed to supply priority-based loads in a hybrid microgrid environment. In Ali et al., 2023, authors investigated the comparison between their proposed grid-connected system and renewable energy-based ad-hoc microgrid to supply critical loads (local hospital). Although these research studies investigated supplying the critical load and presented economic analysis using HOMER, the authors did not provide an in-depth analysis of the resilience enhancement on the variation of investment considering multiple natural disasters. A practical long-term planning strategy should be investigated to enhance the resilience of power systems.

This research work studies resilience-enabling resource adequacy using resilience metrics from planning and operation perspectives. High-fidelity real-time simulations are conducted using Typhoon Hardware In Loop (HIL). The case study is the microgrid facility at the University of Louisiana at Lafayette, USA. The cost of resilience is estimated, and operational limitations are identified in different scenarios of multiple hurricanes. This paper serves as a practical guideline for decision-makers, especially for community energy systems. Our proposed planning scheme will give decision-makers a better insight into what investment is required to improve resilience by a certain level. Resilience studies are always scenario-dependent. Therefore, as step zero, a high-impact, low-frequency event must be identified as the disturbance scenario affecting the system. It largely depends on the geographical area for weather-related events. This paper assumes for every scenario of all the hurricanes that the main power grid is down, and the microgrid is expected to serve the loads solely until the main power grid is restored locally.

So, the main contributions of this paper are given below:

- Introducing a novel framework for optimal energy resilience investments, aligning resources with desired resilience levels to avoid unnecessary redundancy.

- Utilizing a high-fidelity real-time simulator evaluating a campus microgrid's performance in powering local loads during outages, with a focus on resilience enhancement.

- Quantitatively investigating the cost of improving resilience, providing insights into balancing economic considerations with desired energy infrastructure resilience.

The rest of the paper is organized as follows. In section (2), resilience metrics, technical analysis, and economic analysis methods are discussed. Section (3) describes the microgrid as the case study. Results are presented in section (4). Conclusions and future works are presented in sections (5) and (6).

2. Case Study

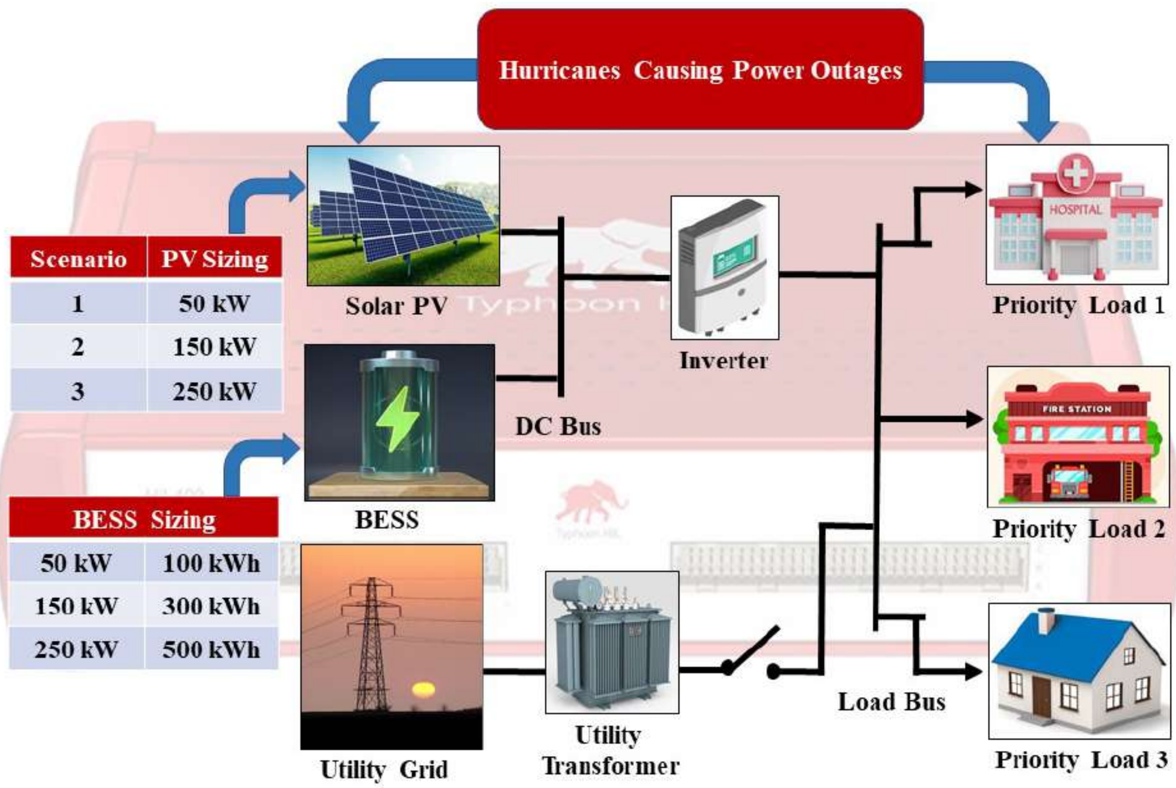

Figure 2: Overview of the UL-Cleco AC/DC Microgrid Facility

The case study in this investigation is a microgrid shown in Fig. 2. Load data from a real distribution feeder is scaled and utilized for three different load categories of this microgrid system. To supply the load demand based on their priority, three load categories are classified as critical load 1, critical load 2, and critical load 3. Here, critical load 1 represents the highest priority for load serving, also labeled as priority load 1; critical load 2 represents the moderate priority for load serving, also labeled as priority load 2; critical load 3 represents the lowest priority for load serving, also labeled as priority load 3. For 24 hours, the total load demand for priority load 1, priority load 2, and priority load 3 is 681.762 kW, 957.701 kW, and 638.475 kW, respectively. The 24-hour load profiles for different priorities are shown in Fig. 3. The simulation has been done considering 24-hour power outages for four hurricanes that hit Louisiana in the past six years. Those hurricanes are Nate (2017), Laura (2020), Zeta (2020), and Ida (2021). For the hurricanes

Laura (2020), Zeta (2020), and Ida (2021), it is considered that the power outages started at 12 am and ran for 24 hours. To investigate from a different dimension, the power outage for Hurricane Nate (2017) is considered to start at 7 am and run for the next 24 hours. To make the investigation more realistic, the solar radiation data corresponding to every hurricane occurring day is collected from the University of Louisiana at Lafayette's 1.1 MW solar PV plant facility Veerendra Kumar et al., 2022. The normalized solar power profile corresponding to each Hurricane day is shown in Fig. 4.

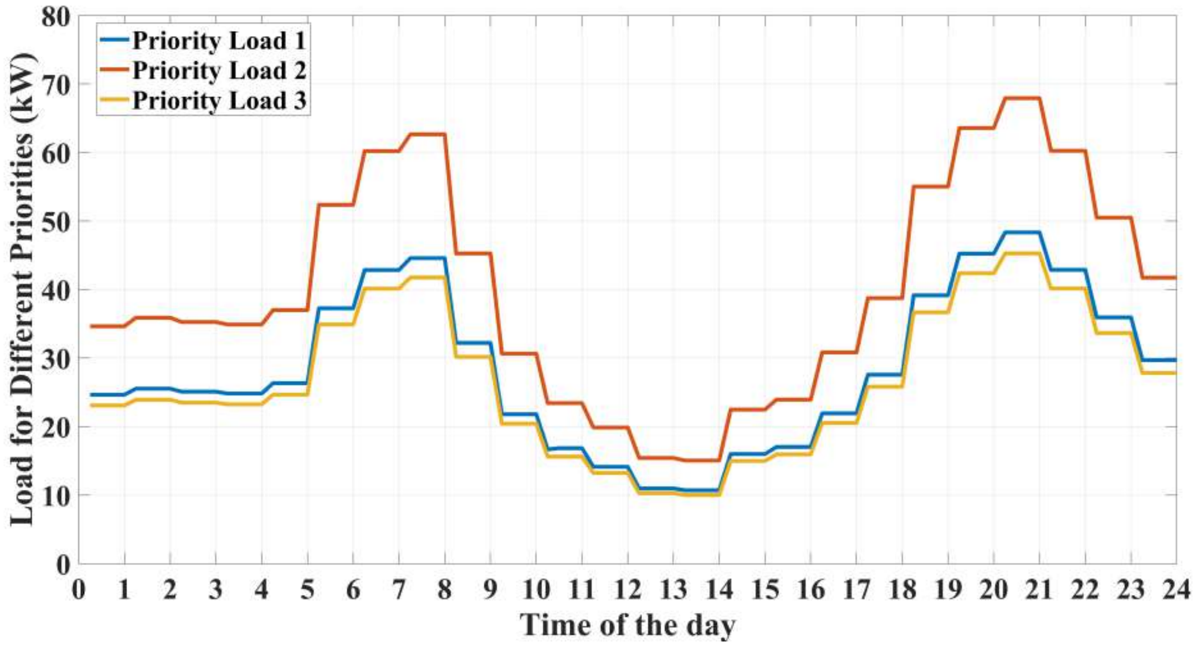

Figure 3: Different Priorities Load Data

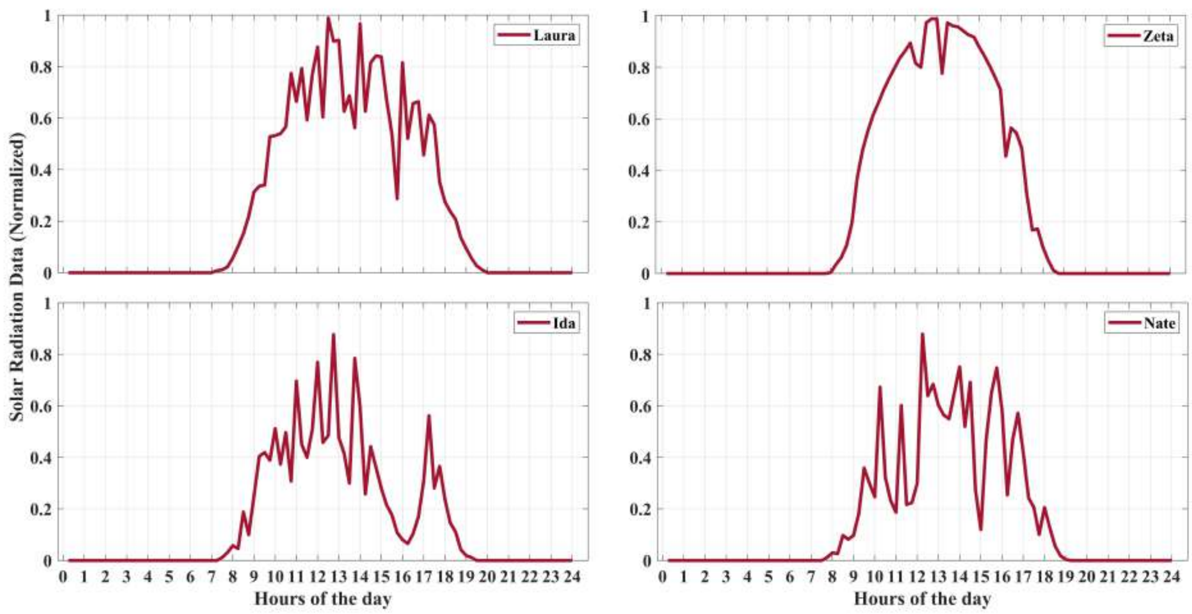

Figure 4: Solar Radiation Data (Normalized)

The microgrid simulation for every hurricane contains three scenarios utilizing three different configurations of solar PV plant and battery energy storage system (BESS). For

Table 1: Configuration of Three Scenarios for Every Hurricanes

Scenario	PV Size	BESS Size (kW)	BESS capacity (kWh)
1	50kW	50kW	100kWh
2	150kW	150kW	300kWh
3	250kW	250kW	500kWh

scenario (I), the solar PV plant is 50 kW, whereas the rating of BESS is 50 kW and 100 kWh. For scenario (II), the solar PV plant is 150 kW, whereas the rating of BESS is 150 kW and 300 kWh. For scenario (III), the solar PV plant is 250 kW, whereas the rating of BESS is 250 kW and 500 kWh. Table 1 contains the simulation configurations of the three scenarios for every hurricane.

The selection of three different PV sizes helps to investigate in detail for enabling three different PV penetration environments. Solar PV penetration is calculated as the ratio of the peak solar photovoltaic power to the peak load apparent power on the feeder Hoke et al., 2012; Ullah et al., 2021.

$$PV\ Penetration = \frac{Peak\ PV\ Power}{Peak\ Load\ Apparent\ Power} \tag{1}$$

Three PV plant sizing is 50kW, 150 kW, 250 kW, and the peak load apparent power is 161.90 KVA. So, using the equation 1, three scenarios of this study represent 30.88%, 92.64%, and 154.41% PV penetration, respectively. For battery capacity, the optimal BESS profit can be generated with 2 kWh of storage capacity per kilowatt peak (kWp) of solar PV system Lund, 2018. So, for three scenarios, BESS size is selected to 100 kWh, 300 kWh, and 500 kWh, respectively. The maximum and minimum state of charge (SOC) for BESS are selected as 90% and 10%, respectively. As we know the probable hurricane arriving day from the weather forecast, it is considered that the BESS is charged and the BESS SOC is 90% when the simulation starts.

To investigate the real-time performance of the microgrid, Typhoon HIL real-time simulator is used to model and analyze the proposed algorithm.

3. Methodology

3.1 Resilience Metrics

During weather-related power outages, it takes several hours to days to restore the main power grid. The formation of microgrids is an effective solution to provide support during power outages. It is realistically impossible to supply all the loads when the main power grid is not operational. Therefore, the loads can be classified based on their priority. Considering 24 hours of power outage for every natural disaster, the served critical loads

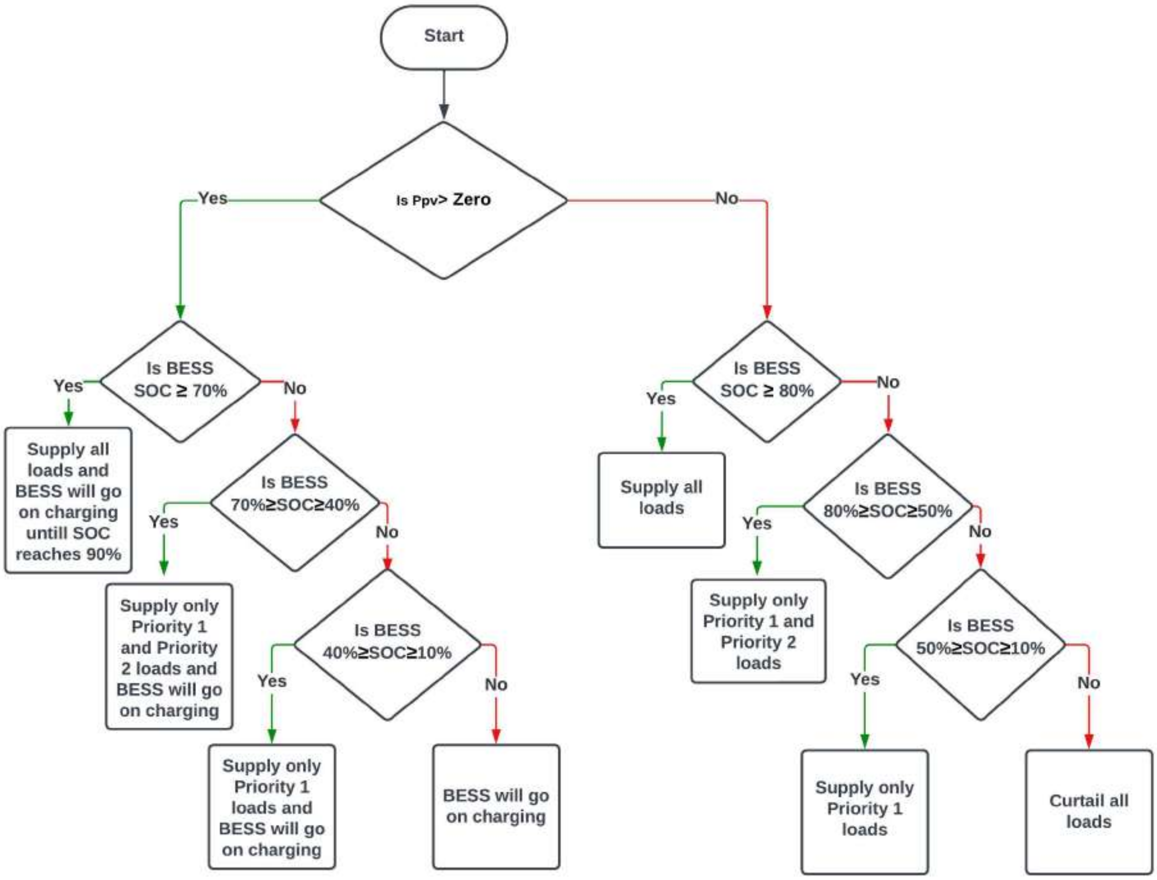

Figure 5: Flowchart of The Microgrid Operation Algorithm

can be calculated and investigated to find out the resilience level of the microgrid.

In our proposed resilience metric, resilience will be evaluated based on the amount of energy supplied to the loads, concentrating on the most critical loads. All the loads will be divided into three categories, where the load groups 1, 2, and 3 will be known as priority load 1, priority load 2, and priority load 3. Here, priority load 1 is the most critical load, priority load 3 is the least critical load, and priority load 2 stays in between them. Researchers investigated resilience enhancement using the value of lost load (VoLL), considering critical loads and non-critical loads. Several recent research studies Gao et al., 2017; Nazemi et al., 2021; Yao, Wang & Zhao, 2018; Yao, Zhao et al., 2018; Yao et al., 2019, 2020 emphasized five times more weight on the most critical loads in comparison to the least critical loads. As priority load 1 is the most critical load and priority load 3 is the least critical load in this study, the weighted factors 5, 2.5, and 1 are assigned for priority load 1, 2, and 3, respectively. So, our proposed resilience metrics can be calculated using the following equation.

$$Resilience, R = 5\alpha_1 + 2.5\alpha_2 + \alpha_3 \tag{2}$$

In (2), α_1 represents conditions of the served load for priority load 1. If priority load 1 is served for a time interval, α_1 will be considered as 1 whereas,α_1 will be considered as 0 if the load is not served. Likewise, α_2, α_3 will be 1 or 0 for priority load 2, and 3, respectively. As α_1, α_2, α_3 maximum value can be 1, the maximum resilience that can be achieved is 8.5. Using our proposed resilience metrics, we can evaluate the resilience level of a power grid (concentrating on the amount of energy served on the most critical loads).

3.2 Technical Analysis

Our proposed algorithm is provided as a flowchart in Fig. 5. The algorithm is designed to satisfy the loads during an outage, concentrating on the most critical load category. This microgrid case study consists of a solar PV plant and battery energy storage system (BESS) to supply different priorities of loads. During the power outage, the solar PV plant and BESS will coordinate to supply the critical loads effectively for a longer duration of hours. During the mid-day or when the solar radiation remains higher for a longer time horizon, it tends to be a more efficient approach to charge the battery to a certain level at first instead of satisfying the less critical load so that the microgrid achieves the ability to supply the critical load 1 during the greater amount of power outage hours. The proposed control system will continuously analyze the solar PV generation, battery state of charge (SOC), and load demands and will take steps accordingly. When there is any solar PV generation, the control system will check the battery SOC conditions and satisfy the load demands based on the battery's SOC. If the battery SOC is greater than 70%, all the load demands will be fulfilled by solar PV and BESS. If solar PV generation is higher than all the load demands, solar PV will satisfy the power demands by itself, and the extra generated PV power will go to the battery for its charging. If the solar-generated power is less than the power demands of all the loads, solar PV and battery storage systems will satisfy the load demands together. When the battery SOC remains in the range between 70% to 40%, only priority loads 1 and 2 will be served, and priority load 3 will be cut off. If solar PV generation is higher than the demands of priority loads 1 & 2, solar PV will satisfy the power demands by itself, and the extra generated PV power will go to the battery for its charging. Otherwise, solar PV and battery storage systems will satisfy the load demands together. When the battery SOC remains between 40% to 10%, only priority load 1 will be satisfied, whereas priority loads 1 & 2 will be curtailed. If solar PV generation is higher than the demands of priority loads 1, solar PV will satisfy the power demands by itself, and the extra generated PV power will go to the battery for its charging. Otherwise, solar PV and battery storage systems will satisfy the load demands together. If the battery SOC is less than 10%, all the priority loads will be curtailed, and the battery will go to charging mode solely.

When there is no solar PV generation, the battery will satisfy the loads. If the battery SOC remains higher than 80%, all the loads will be supplied. If the SOC stays between 80% to 50%, only the priority loads 1 & 2 will be supplied while priority load 3 will be cut off. When the SOC remains in the range of 50% to 10%, only priority load 1 will be served, whereas priority loads 2 & 3 will not be satisfied. If the battery SOC go below 10%, all the loads will be curtailed.

3.3 Economic Analysis

This research studies the economic assessment from different perspectives of economic indicators. 25 years is considered as the average life duration of solar PV panels Anusuya et al., 2023; Chowdhury et al., 2020; Tan et al., 2022. A solar PV power generation-based project consists of design, building, and operation of a solar PV power plant for a time period of 20-30 yearsCurtis et al., 2021. In this study, a 24-year time horizon is selected for the economic assessment of this microgrid studyUllah et al., 2023. The time duration of solar PV inverter and BESS is 12 years and 10 years, respectivelyMongird et al., 2020; Ramasamy et al., 2022. In this investigation, 8 years is selected as the time duration of the solar PV inverter and BESS as the advanced features (i.e., Volt-VAR control, Volt-Watt control, etc.) shorten the inverter's conventional lifetime Gandhi et al., 2018. Cost analyses are provided for all three scenarios of the four hurricanes. Furthermore, the investigation is also extended to analyze the impact of the increased number of Hurricanes in a 24-year time horizon (considering 4 hurricanes in 1 set).

The revenue is produced from the selling of solar plus storage power to the priority loads 1, 2, and 3. Using 3, the revenue, R can be found where E_i represents the energy supplied to the priority loads in kWh, and α is the selling price of solar plus storage energy in \$/kWh. Inflation factor, d is considered as 2.5% for this investigation Ramasamy et al., 2022. During the hurricane days emergency supply, the value of α is considered as \$10/kWh, \$5/kWh, and \$2/kWh for priority load 1 (most critical load), priority load 2 (medium critical load), and priority load 3 (least critical load), respectively Nazemi et al., 2021; Yao, Wang & Zhao, 2018; Yao, Zhao et al., 2018; Yao et al., 2019, 2020. For all the remaining regular days, the value of α is considered as \$0.10/kWh in this case study.

$$R = \sum_{i=1}^{n} E_i \cdot \alpha \cdot (1 + d)^{i-1} \tag{3}$$

Equation 4 calculates the expenditure of the solar PV system which is the algebraic summation of the market price of the solar PV panel, C_{PV}^{MAR}, operation and maintenance cost of the solar, C_{PV}^{OM}, and salvage value of the solar PV, C_{PV}^{SAL}. Equation 5 calculates the expenditure of the solar PV inverter, which is the algebraic summation of the market price of the inverter, C_{INV}^{MAR}, operation and maintenance cost of the inverter, C_{INV}^{OM}, salvage value of the solar inverter, C_{INV}^{SAL}. Equation 6 is used to compute total inverter expenditure for 24 years time period where S_{INV} is the rating of the inverter in kVA, d is the inflation factor, and T_R^{INV} is the lifetime of the inverter.

$$C_{PV} = C_{PV}^{MAR} + C_{PV}^{OM} - C_{PV}^{SAL} \tag{4}$$

$$\beta = C^{MAR}_{PV,INV} + C^{OM}_{PV,INV} - C^{SAL}_{PV,INV} \tag{5}$$

$$C_{PV,INV} = \sum_{j=1}^{n} S_{INV} \cdot \beta \cdot (1+d)^{(\frac{T_R^{INV}}{2})(j-1)} \tag{6}$$

The BESS expenditure is calculated based on its power and energy ratings using equation 7 and 8, respectively. Equation 7 is used to determine the BESS cost for power rating, γ, which is the algebraic summation of the market price of BESS for power rating, $C^{MAR}_{BESS,P}$, O&M cost of the BESS for power rating,$C^{OM}_{BESS,P}$, and the salvage value of BESS for power rating, $C^{SAL}_{BESS,P}$. Equations 8 is used to calculate the BESS cost for energy rating, η, and this calculation follows the same approach of the equation 7. η is determined using the market price of BESS for energy rating, $C^{MAR}_{BESS,E}$, O&M cost of the BESS for energy rating,$C^{OM}_{BESS,E}$, and the salvage value of BESS for energy rating, $C^{SAL}_{BESS,E}$. In equation 9, BESS cost for 24 years is calculated where the BESS lifetime, T_R^{BESS}, is considered as 8 years, and p is the BESS depreciation rate for each year, 2%. P_{BESS}, and E_{BESS} represent the power capacity and energy capacity of the battery, respectively. To calculate the battery inverter cost, equation 10 is utilized where the cost of the BESS inverter is the algebraic summation of the market price of the BESS inverter, $C^{MAR}_{BESS,INV}$, operation and maintenance cost of the BESS inverter, $C^{OM}_{BESS,INV}$, salvage value of the BESS inverter, $C^{SAL}_{BESS,INV}$.

$$\gamma = C^{MAR}_{BESS,P} + C^{OM}_{BESS,P} - C^{SAL}_{BESS,P} \tag{7}$$

$$\eta = C^{MAR}_{BESS,E} + C^{OM}_{BESS,E} - C^{SAL}_{BESS,E} \tag{8}$$

$$C_{BESS} = \sum_{k=1}^{n} [\gamma \cdot P_{BESS} + \eta \cdot E_{BESS}] \cdot (1-p)^{(T_R^{BESS}-1)(k-1)} \tag{9}$$

$$\delta = C^{MAR}_{BESS,INV} + C^{OM}_{BESS,INV} - C^{SAL}_{BESS,INV} \tag{10}$$

$$C_{BESS,INV} = \sum_{j=1}^{n} S_{BESS,INV} \cdot \delta \cdot (1+d)^{(\frac{T_R^{INV}}{2})(j-1)} \tag{11}$$

In table 2, all the input parameters of economic analysis and their corresponding values are included. Here, we presented some economic indicators that measure the benefit of solar plus storage systems in power distribution systems for 24 years operation horizon.

1. **Total cost**: the Total cost, C, is the summation of costs for solar PV panel, solar PV inverter, BESS, and BESS inverter expressed in 12.

$$C = C_{PV} + C_{PV,INV} + C_{BESS} + C_{BESS,INV} \tag{12}$$

2. **Gained profit by solar system's owner**: The profit, P is the difference between the revenue and the total cost calculated using the equation 13. The revenue, R, expressed in the equation 3.

$$P = R - C. \tag{13}$$

3. **Net Profit Margin**: The net profit margin NPM, or simply net margin, represents how much net income or profit is generated as a percentage of revenue made by solar system owner. The ratio represents the net profit to revenue for the owner of a solar system facility.

$$NPM = \frac{P}{R} \tag{14}$$

4. **Net Present Value**: Two terms characterize the net present value (NPV), the present discounted value of costs PDC in (16) and the present discounted value of revenues PDR in (15) by $NPV = PDR - PDC$. If we consider R_i to be the (undiscounted) revenues (benefits) of the solar system project during the year i and we consider C_i to be the (undiscounted) costs of the solar system project during the year i, afterward, we can calculate NPV using equation (17). When the NPV is more than zero, the investment plan is considered as profitable from the investor side.

$$PDR = \sum_{i=1}^{T} \frac{R_i}{(1+d)^{i-1}} \tag{15}$$

$$PDC = \sum_{i=1}^{T} \frac{C_i}{(1+d)^{i-1}} \tag{16}$$

$$NPV = \sum_{i=1}^{T} \frac{(R_i - C_i)}{(1+d)^{i-1}} \tag{17}$$

5. **Revenue-Cost Ratio**: The revenue-cost ratio is the ratio of PDR to PDC which is mentioned in (18). When the RCR is greater than one, the investment plan will make revenue for the investor.

$$RCR = \frac{PDR}{PDC} = \frac{\sum_{i=1}^{T} \frac{R_i}{(1+d)^{i-1}}}{\sum_{i=1}^{T} \frac{C_i}{(1+d)^{i-1}}} \tag{18}$$

Table 2: Different Input Parameters of Economic Analysis

Parameters	Value	Reference
α	10, 5, 2, 0.1 (\$/kWh)	Nazemi et al., 2021; Yao, Wang & Zhao, 2018; Yao, Zhao et al., 2018; Yao et al.,
d	2.5%	Ramasamy et al., 2022
C_{PV}^{MAR}	400 (\$/kW)	Ramasamy et al., 2022
C_{PV}^{OM}	1% (\$/kW)	Deotti et al., 2020
C_{PV}^{SAL}	10% (\$/kW)	Humphreys & Brown, 1990
C_{INV}^{MAR}	60 (\$/kW)	Ramasamy et al., 2022
C_{INV}^{OM}	1% (\$/kW)	
C_{INV}^{SAL}	10% (\$/kW)	Humphreys & Brown, 1990
$C_{BESS,INV}^{MAR}$	50 (\$/kW)	Ramasamy et al., 2022
$C_{BESS,INV}^{OM}$	1% (\$/kW)	
$C_{BESS,INV}^{SAL}$	10% (\$/kW)	Humphreys & Brown, 1990
$C_{BESS,P}^{MAR}$	628 (\$/kW)	Ramasamy et al., 2022
$C_{BESS,P}^{OM}$	10 (\$/kW)	Mongird et al., 2020
$C_{BESS,P}^{SAL}$	10% (\$/kW)	Humphreys & Brown, 1990
$C_{BESS,E}^{MAR}$	157 (\$/kW)	Ramasamy et al., 2022
$C_{BESS,E}^{OM}$	0.003 (\$/kW)	Mongird et al., 2020
$C_{BESS,E}^{SAL}$	10% (\$/kW)	Humphreys & Brown, 1990
E_{BESS}	100, 300, 500 (kWh)	
P_{BESS}	50, 150, 250 (kW)	
p	2%	
S_{INV}	55, 162, 275 kVA	
T_R^{INV}	8 Years	
T_R^{BESS}	8 Years	

4. Results and Discussion

In this section, the results of the resilience metrics, technical analysis, and economic analysis are presented and analyzed. All the simulation results are collected from the real-time simulator Typhoon HIL for its high-fidelity characteristics.

4.1 Resilience Metrics

After the completion of microgrid simulation for all the scenarios considering all power outages caused by the hurricanes, the resilience curve of all scenarios for all the power outages is plotted for 24 hours. In Fig. 6, the resilience curve for three scenarios is plotted for a 24-hour power outage due to Hurricane Laura, which runs from 12 am to 12 am. From 2 am to 8:45 am and 6:45 pm to 12 am, the resilience value remains zero for scenario 1; during these time intervals, solar PV and BESS cannot serve any load at all. From 12 am to 2 am and 8:45 am to 6:45 pm, different priority loads are satisfied in scenario 1. It is important to mention that scenario 1 resilience value remains zero for a longer period of time in comparison with scenario 2 & 3 (scenarios 1, 2, 3 configuration is already provided in Table 1). Although scenario 2 contains a resilience value of zero from 6 am to 8:15 am and from 9 pm to 12 am, it shows a resilience value of zero for 5.25 hours whereas scenario 1 shows it for 12 hours. Scenario 3 shows a higher resilience trend than scenario 1 and scenario 2 for the significant time duration during the 24-hour time horizon. The resilience values of scenario 3 also show that energy is supplied to the most critical load during the whole 24 hours without curtailing any priority load 1. The lowest resilience value of scenario 3 is 5, whereas the lowest resilience values of scenario 1 and scenario 2 stay zero for 12 and 5.25 hours, respectively. Scenario 3 shows the best resilience curve where the solar PV and BESS successfully served the most critical load for a 24-hour time horizon. The results show the extent to which resilience is improved with a certain investment in resources.

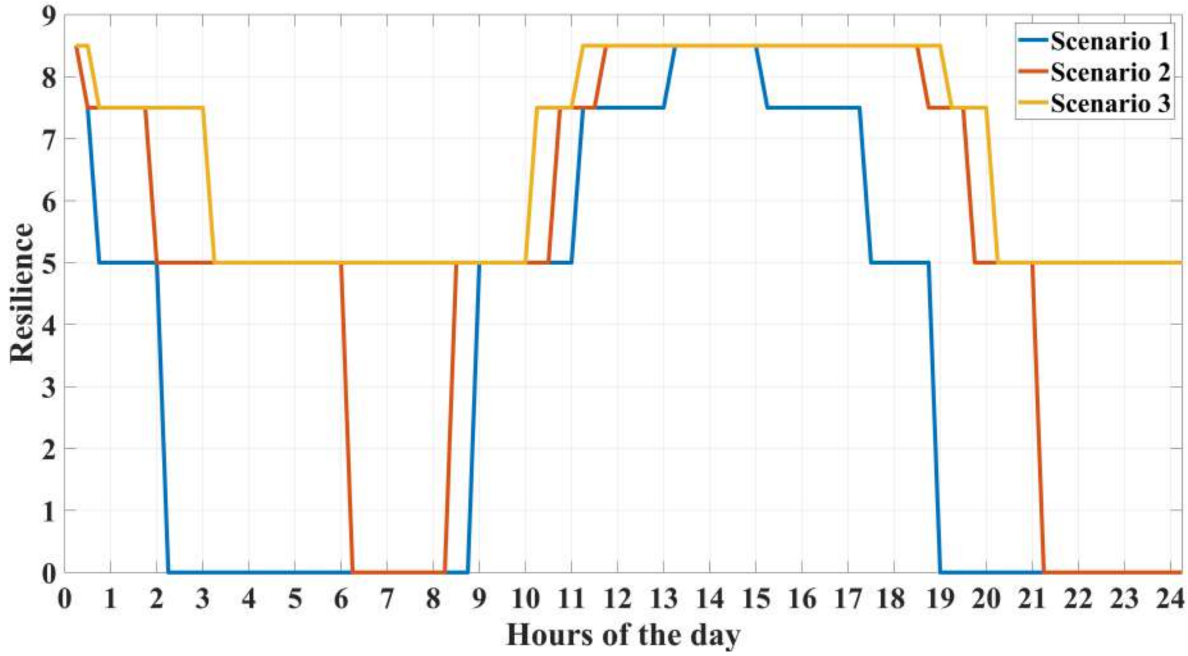

Figure 6: Resilience evaluation for the hurricane Laura

In Fig. 7, the resilience value for three scenarios is plotted for a 24-hour power outage due to Hurricane Zeta. From 2 am to 9 am and from 6.15 pm to 12 am, the resilience value remains zero for scenario 1. Moreover, scenario 1 resilience value remains zero for maximum outage hours among all three scenarios. Although scenario 2 contains a resilience value of zero from 6 am to 8:45 am and from 9:15 pm to 12 am, it shows zero resilience value for only 5.5 hours whereas scenario 1 holds zero resilience value for 12.75 hours, indicating more than 50% improvement in scenario 2. Scenario 3 shows a higher resilience trend than scenario 1 and scenario 2 for the significant time of the 24-hour time horizon. The resilience values of Scenario 3 also show that energy is supplied to the most critical load almost all 24 hours except from 8 am to 8:30 am and from 23:45 pm to 12 AM when the resilience value of scenario 3 becomes 0. It is worth mentioning that scenario 3 configuration of solar PV and BESS also served priority loads 2 & 3 much better than scenario 1 & 2.

In Fig. 8, the resilience value for three scenarios is plotted for a 24-hour power outage due to Hurricane Ida. From 2 am to 8:45 am and from 6 pm to 12 am (except the in-between time duration of 7:45 pm to 8 pm), the resilience value remains zero for scenario

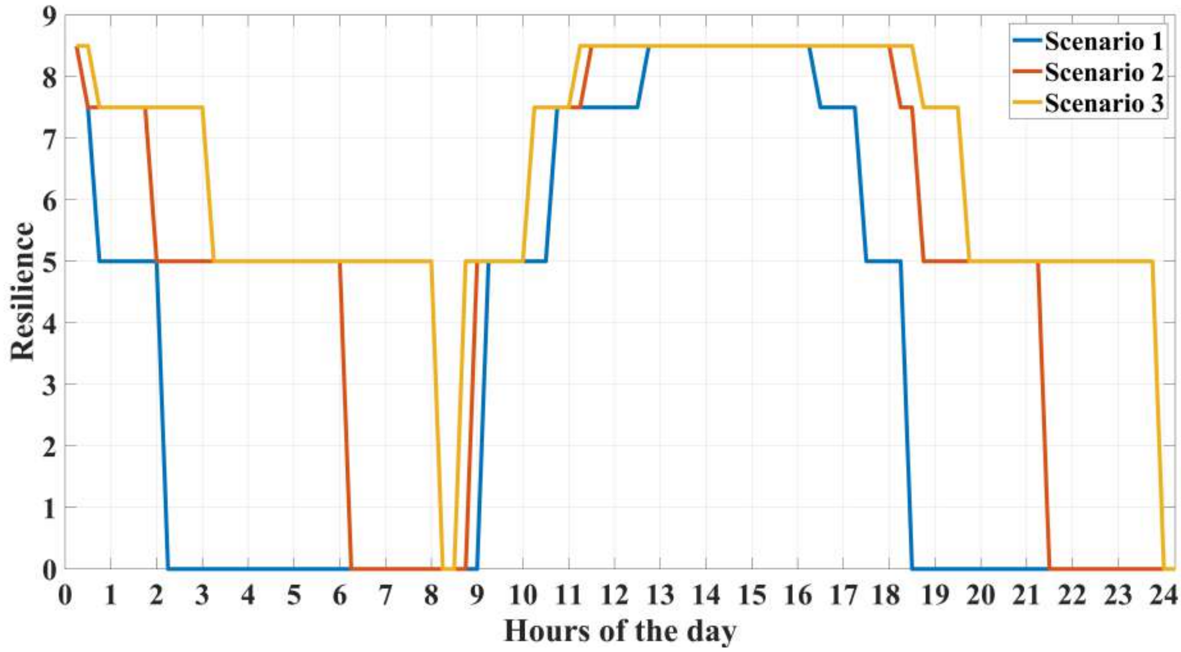

Figure 7: Resilience evaluation for the hurricane Zeta

1. Moreover, scenario 1 resilience value remains zero for maximum outage hours among all three scenarios. Although scenario 2 contains a resilience value of zero from around 6 am to around 8:15 am and from 8:30 pm to 12 am, it shows a resilience value of zero for only 5.75 hours, whereas scenario 1 shows 12.75 hours. Scenario 3 shows a higher resilience value characteristics than Scenario 1 and Scenario 2 for the significant time of the 24-hour time horizon. The resilience values of scenario 3 also show that energy is supplied to the most critical load for all 24-hour power outages without any curtailment of the most critical load.

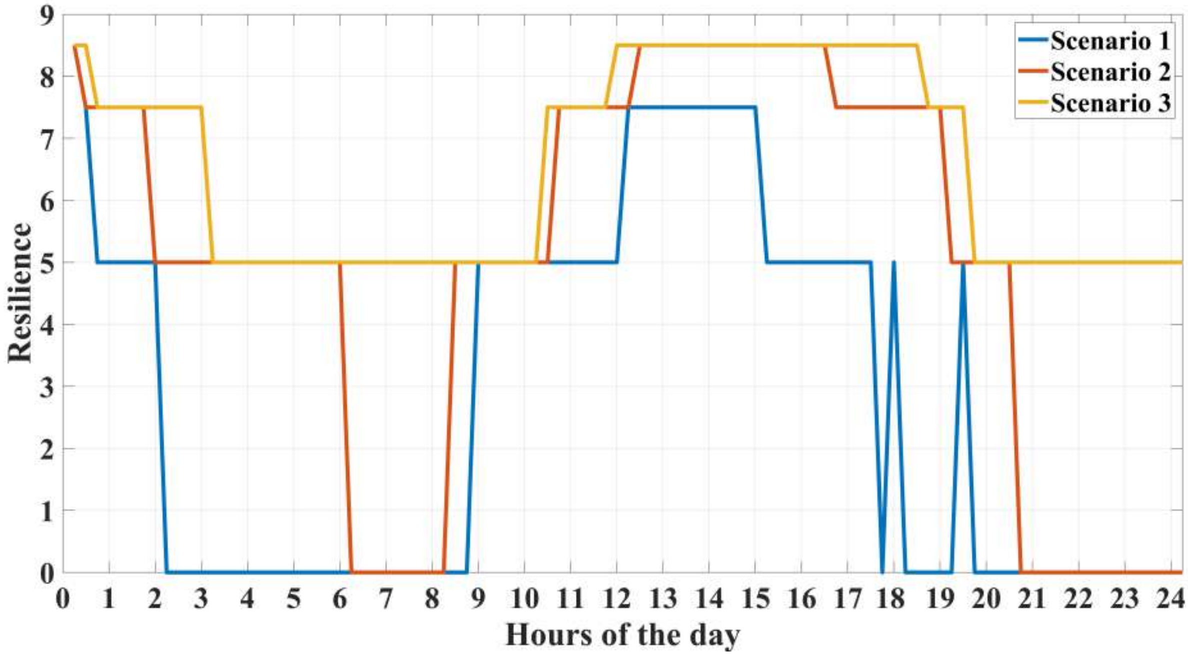

Figure 8: Resilience evaluation for the hurricane Ida

In Fig. 9, the resilience value for three scenarios is plotted for 24-hour power outages due to Hurricane Nate. From 8 am to 9 am and from 6.15 pm to 7 am, which represents 13.75 hours of the 24-hour time period, the resilience value remains zero for scenario 1. Moreover, the scenario 1 resilience value remains zero for the maximum number of outage hours among all the scenarios. Although scenario 2 contains a resilience value of zero from 9 pm to 7 am, it contains a resilience value of zero for 10 hours, whereas scenario 1 has zero resilience values for 13.75 hours . Scenario 3 shows a higher resilience value than scenario 1 and scenario 2 for the significant time of the 24-hour time horizon. The resilience values of Scenario 3 also show that energy is supplied to the most critical load successfully from 7 AM to 12 AM, whereas from 12:15 am to 7 am, for 6.75 hours, the resilience value of scenario 3 remains 0. Although scenario 3 of Hurricane Nate could not supply energy to the most critical load for 6.75 hours, which is the worst performance among all scenarios 3 of four hurricanes, still scenario 3 configuration of the power outages caused by Hurricane Nate shows better performance in serving the most critical load 7 hours more than scenario 1 and 3.25 hours more than scenario 2.

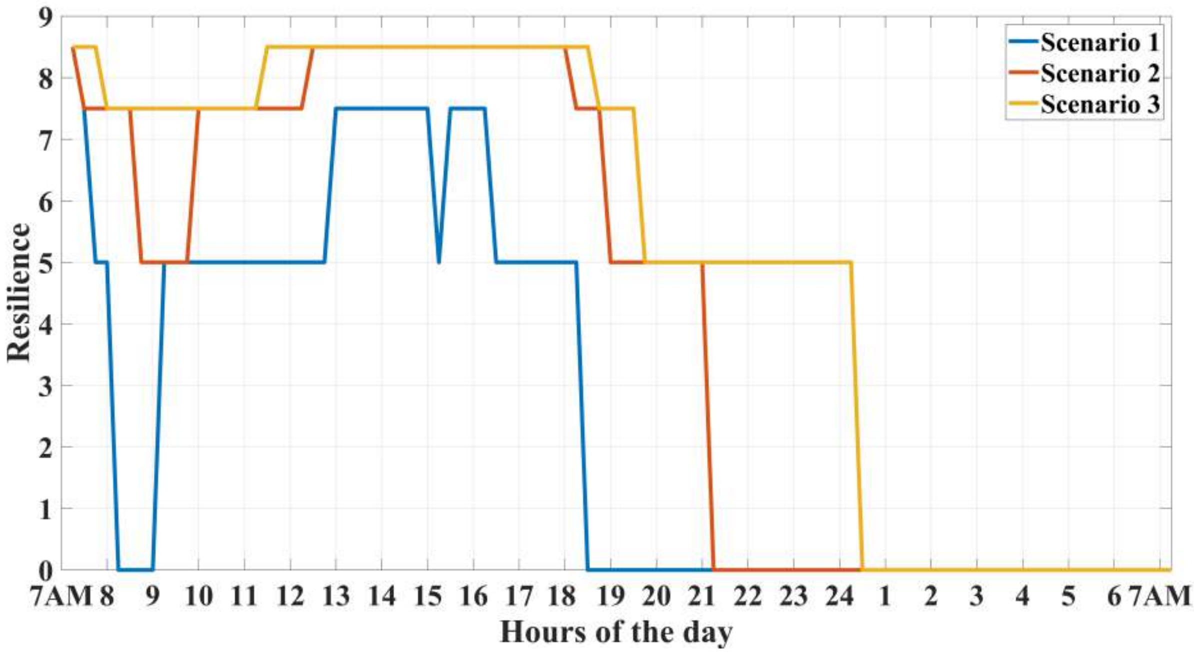

Figure 9: Resilience evaluation for the hurricane Nate

4.2 Technical Analysis

In this section, the served amount of different critical loads for all the scenarios of power outages will be described and analyzed. In Fig. 10, the served load of Priority Loads 1, 2, and 3 are illustrated for all three scenarios of power outages due to Hurricane Laura. For priority load 1, 35.89% of loads are served in scenario 1, whereas 70.07% loads are served in scenario 2. In scenario 3, all the 100% priority load 1 is served successfully during the whole 24 hours. For priority load 2, 16.15% loads are served in scenario 1, whereas 34.09% loads are served in scenario 2. In scenario 3, 43.25% of priority load 2 is

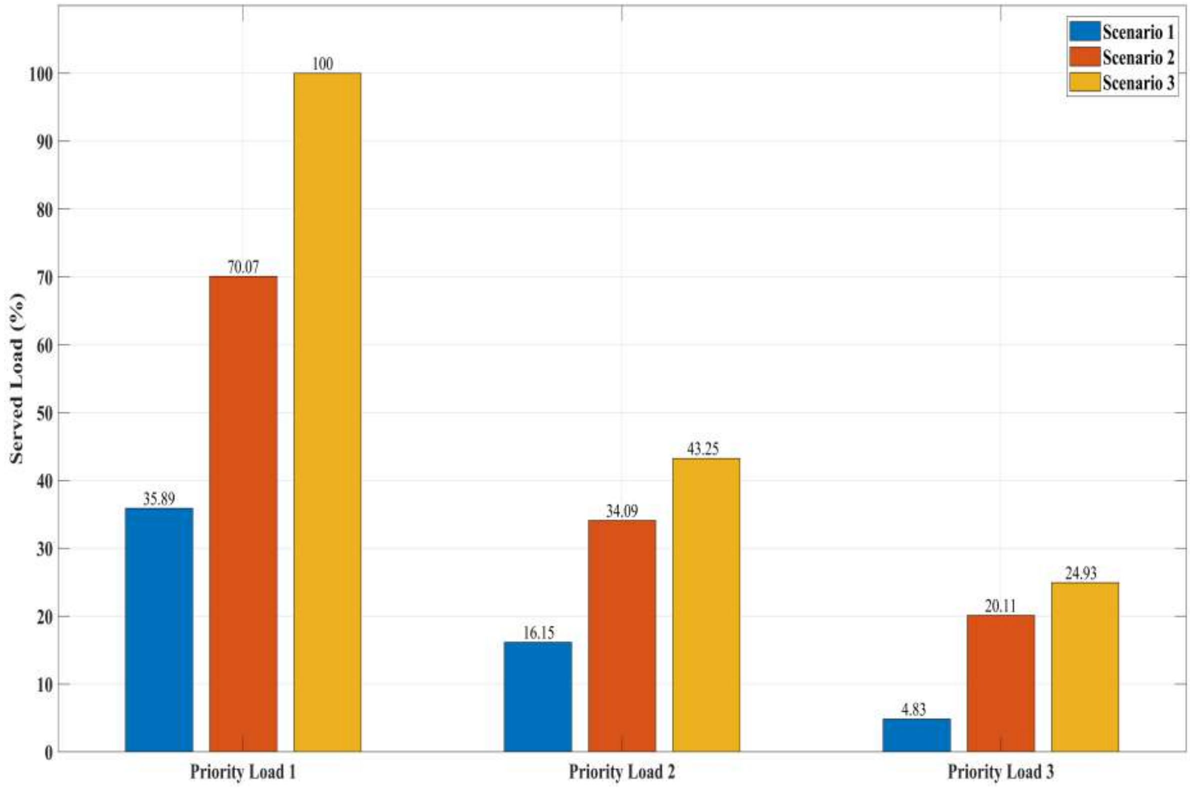

Figure 10: Served Loads for the Hurricane Laura (In Percent)

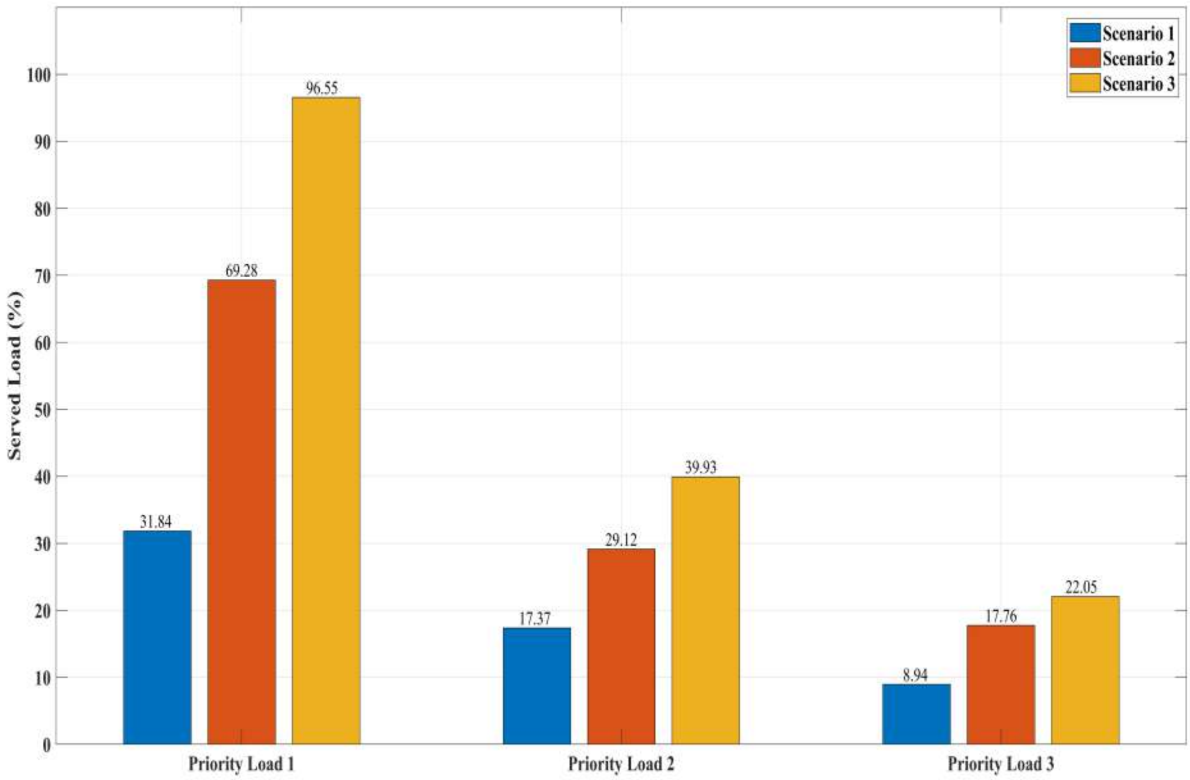

Figure 11: Served Loads for the Hurricane Zeta (In Percent)

served. For priority load 3, 4.83%, 20.11%, and 24.93% of loads are served in scenarios 1, 2, and 3, respectively. During all three scenarios, there is a trend of increasing served load for all the priority loads. Most importantly, the amount of served loads of priority

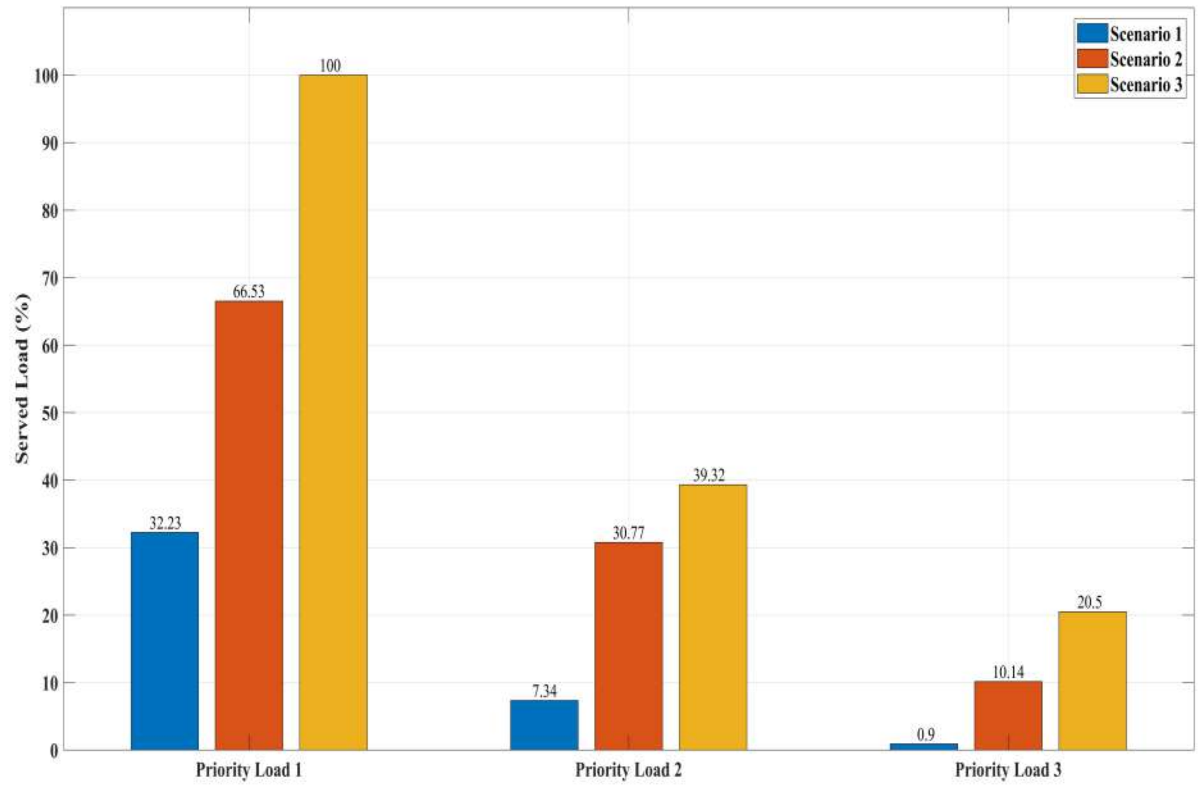

Figure 12: Served Loads for the Hurricane Ida (In Percent)

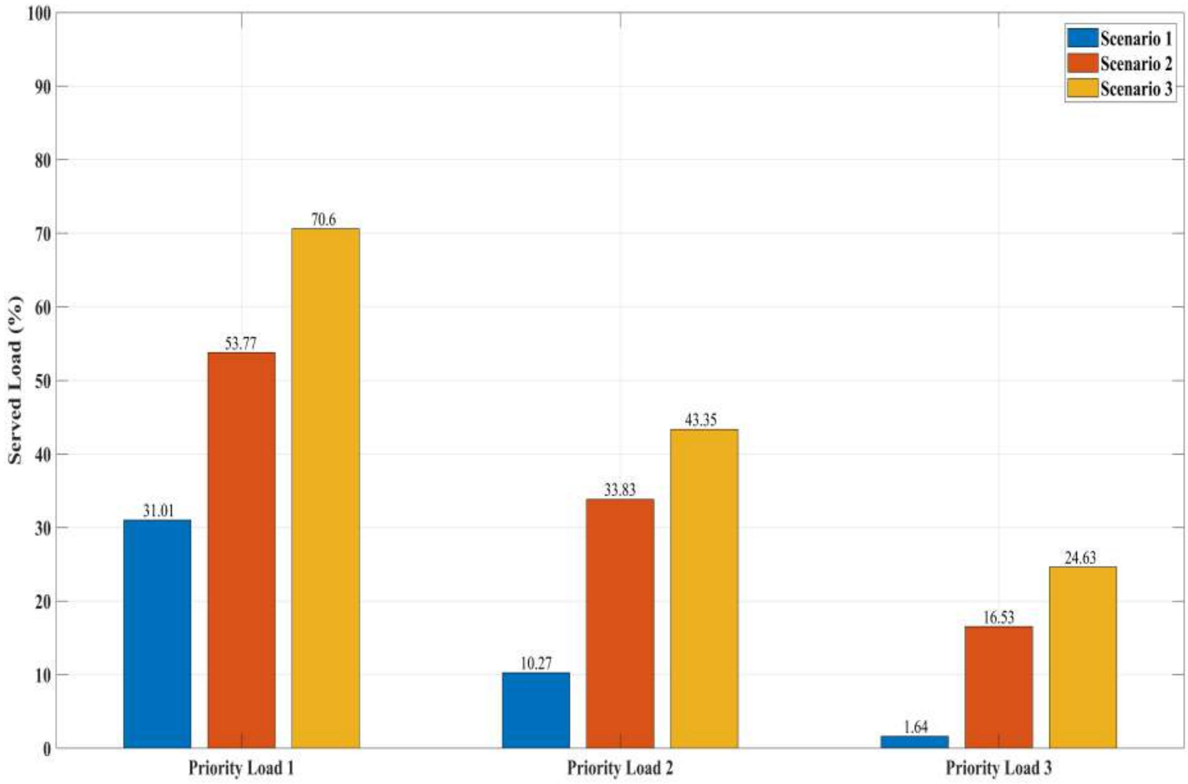

Figure 13: Served Loads for the Hurricane Nate (In Percent)

load 1 doubled in scenario 2 in comparison to scenario 1, whereas scenario 3 shows the best performance by satisfying 100% priority load 1, which is the most critical load.

In Fig. 11, the served load of Priority Loads 1, 2, and 3 are depicted for all three

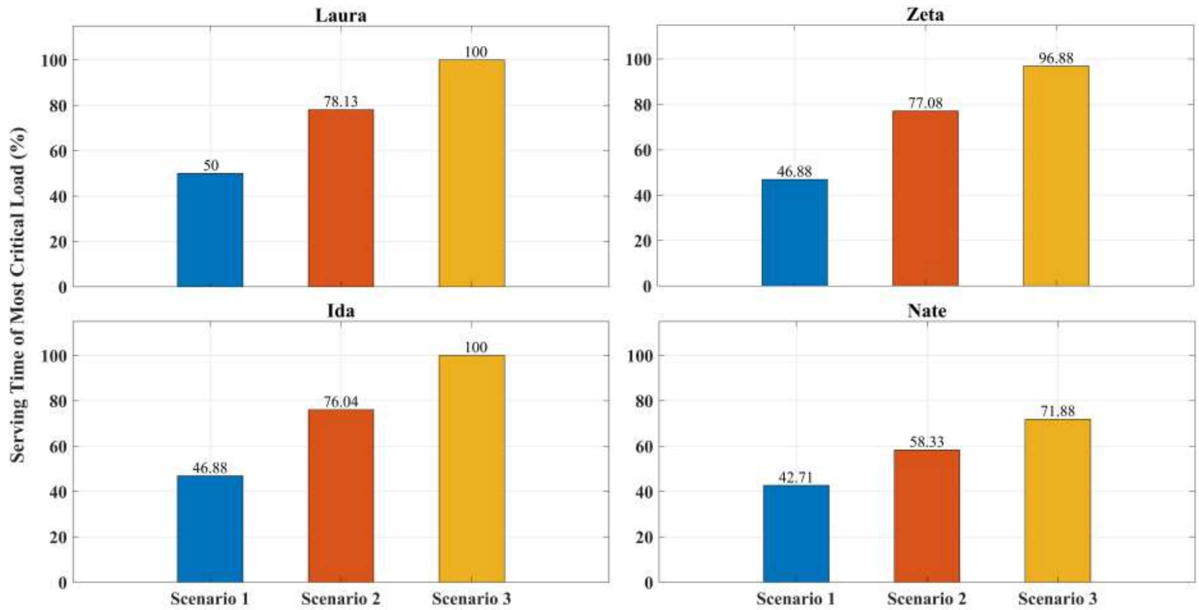

Figure 14: Serving Time Duration of Most Critical Load (In Percent)

scenarios of power outages caused by Hurricane Zeta. For priority load 1, 31.84% loads are served in scenario 1, whereas 69.28% loads are served in scenario 2. In scenario 3, 96.55% priority load 1 is served during the whole 24 hours. For priority load 2, 17.37% loads are served in scenario 1, whereas 29.12% loads are served in scenario 2. In scenario 3, 39.93% of priority load 2 is served. For priority load 3, 8.94%, 17.76%, and 22.05% of loads are served in scenarios 1, 2, and 3, respectively. During all three scenarios, there is also a similar trend of increasing served load for all the priority loads, like Hurricane Laura. For priority load 1, the amount of served loads of priority load 1 is more than doubled in scenario 2 in comparison to scenario 1, whereas scenario 3 shows the best performance by serving 96.55% priority load 1, which is the main objective of our proposed control system. For the outage caused by Hurricane Zeta, the solar PV plant received solar radiation 45 minutes later in the early morning in comparison to the power outages caused by Hurricane Laura, which is the major reason for satisfying 96.55% most critical load. If the solar radiation would come earlier in the morning, the solar PV plant could start generating solar PV power earlier, and BESS could also go into charging mode, which could help to achieve 100% satisfaction of most critical loads like the previous case study of power outages by Hurricane Laura.

In Fig. 12, the served load of Priority Loads 1, 2, and 3 are drawn for all three scenarios of power outages caused by Hurricane Ida. For priority load 1, 32.23% loads are served in scenario 1, whereas 66.53% loads are served in scenario 2. In scenario 3, all the 100% priority load 1 demand is satisfied successfully during the whole 24 hours. For priority load 2, 7.34% loads are served in scenario 1, whereas 30.77% loads are served in scenario 2. In scenario 3, 39.32% of priority load 2 is served. For priority load 3, 0.9%, 10.14%, and 20.50% of loads are served in scenarios 1, 2, and 3, respectively. During all three scenarios, there is a trend of increasing served load for all the priority loads.

Most importantly, the amount of served loads of priority load 1 is more than doubled in scenario 2 in comparison to scenario 1, whereas scenario 3 shows the best performance by satisfying 100% of the most critical load demand. For the outage caused by Hurricane Ida, the solar PV plant received earlier solar radiation than Hurricane Zeta but later than Hurricane Laura. So, this helped in satisfying 100% of the most critical load in scenario 3, like Hurricane Laura. Although the most critical load is satisfied 100% in scenario 3 of Hurricane Ida, the satisfaction of priority load 3 is lowest in comparison to Hurricane Laura and Hurricane Zeta. In comparison to Hurricane Laura and Hurricane Zeta, the lower peak value of solar radiation throughout the power outage caused by Hurricane Ida is the main reason for the lower satisfaction of priority load 3.

In Fig. 13, the served load of Priority Loads 1, 2, and 3 are drawn for all three scenarios of power outages caused by Hurricane Nate. For priority load 1, 31.01% loads are served in scenario 1, whereas 53.77% loads are served in scenario 2. In scenario 3, 70.6% priority load 1 demand is satisfied. For priority load 2, 10.27% loads are served in scenario 1, whereas 33.83% loads are served in scenario 2. In scenario 3, 43.35% of priority load 2 is served. For priority load 3, 1.64%, 16.53%, and 24.63% of loads are served in scenarios 1, 2, and 3, respectively. During all three scenarios, there is a trend of increasing served load for all the priority loads like all the other hurricanes. Most importantly, the amount of served loads of priority load 1 is 22% higher in scenario 2 in comparison to scenario 1, whereas scenario 3 shows the best performance by satisfying 70.6% priority load 1 demand, which is almost double in comparison to scenario 1. Although the solar PV plant received early solar radiation in morning and received moderate peak solar radiation throughout the power outages caused by Hurricane Nate, the different approach (investigating from 7 am to 7 am next day, unlike the previous 3 hurricanes time duration from 12 am to 12 am next day) played the major reason for satisfying the lowest amount of most critical load among all the four hurricanes. The power outages caused by Hurricane Nate occurred from 7 am to 7 am the next day for 24 hours. Although BESS stays in a healthy condition from 7 am to 7 pm, it can not get any charging opportunities in the next 12 hours. On the other hand, all the previous 3 hurricanes, BESS discharges from 12 am to 7 am(when there is no solar PV generation) and gets opportunities for charging for the next 12 hours(from 7 am to 7 pm), which essentially helps BESS to supply in the dark hours(when there is no sunlight, from 7 pm to 12 am).

Our proposed algorithm fully prioritizes satisfying the priority load 1 (most critical load) throughout the time horizon. In Fig. 14, the time duration of the served most critical load is presented. For Hurricane Laura, the most critical load is satisfied for 50% hours of the 24 hours in scenario 1, whereas the most critical load is served in scenario 2 for 78.13% hours of the 24 hours. Scenario 3 shows the best performance by satisfying the most critical load for the whole 24 hours. For Hurricane Zeta, the most critical load is satisfied for 46.88% hours of the 24 hours in scenario 1, whereas the most critical load is served in scenario 2 for 77.08% hours of the 24 hours. Scenario 3 shows the best performance by satisfying the most critical load for around 96.88% time of the whole 24 hours. For Hurricane Ida, the most critical load is satisfied for 46.88% hours of the 24 hours in scenario 1, whereas the most critical load is served in scenario 2 for 76.04% hours of the 24 hours. Scenario 3 shows the best performance by satisfying the most critical load for the whole 24 hours. For Hurricane Nate, the most critical load is satisfied for around 42.71% hours of the 24 hours in scenario 1, whereas the most critical load is served in scenario 2 for 58.33% hours of the 24 hours. Scenario 3 shows the best performance by satisfying the most critical load for 71.88% hours of the 24 hours. Among all the hurricanes, Scenario 3 shows best performance in comparison to Scenario 1 & 2.

In Fig. 15, Fig 16, Fig 17, and Fig18, the battery SOC profiles for all the scenarios of the hurricanes are presented. In Fig. 15, the battery SOC for all three scenarios is provided for Hurricane Laura. In scenario 1, the battery SOC stays at 10% for around 10 hours, which is the maximum duration of hours in all the scenarios. 10% SOC indicates that no loads are served during that time horizon. In scenario 2, the battery SOC shows better characteristics, and SOC stays at 10% for around 4 hours. The SOC stays at 90% for around 6 hours, indicating that all the loads are served during that time. In scenario 3, the minimum SOC never reaches 10% ,and the minimum SOC is 12.05%, which shows that at least priority load 1 is served for the whole 24 hours. The SOC remains 90% for more than 6 hours, indicating that all the loads are served during that time.

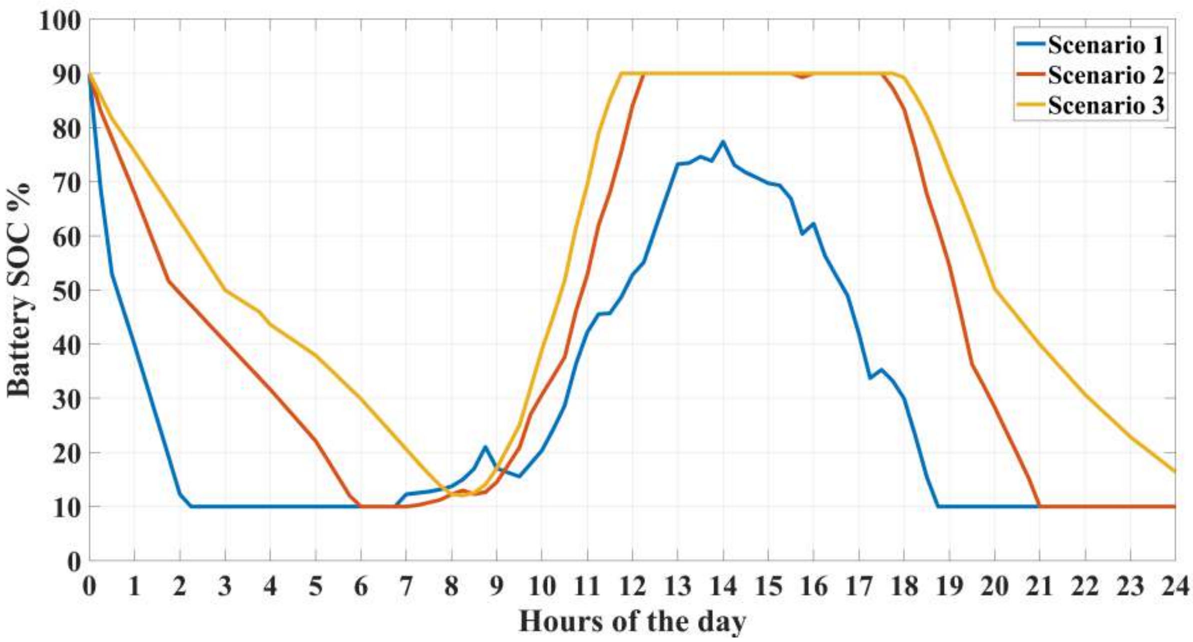

Figure 15: Battery SOC for the Hurricane Laura

In Fig. 16, the battery SOC for all three scenarios is provided for Hurricane Zeta. In scenario 1, the battery SOC stays at 10% for around 11 hours, which is the maximum duration of hours in all the scenarios. In scenario 2, the battery SOC shows better characteristics, and SOC stays at 10% for around 5 hours. The SOC stays at 90% for around 5 hours, indicating that all the loads are served during that time. In scenario 3, the minimum SOC reaches 10% for less than an hour in the whole 24 hours, which shows that at least priority load 1 is served for almost all 24 hours. The SOC stays 90% for more than 5.5 hours, indicating that all the loads are served during that time.

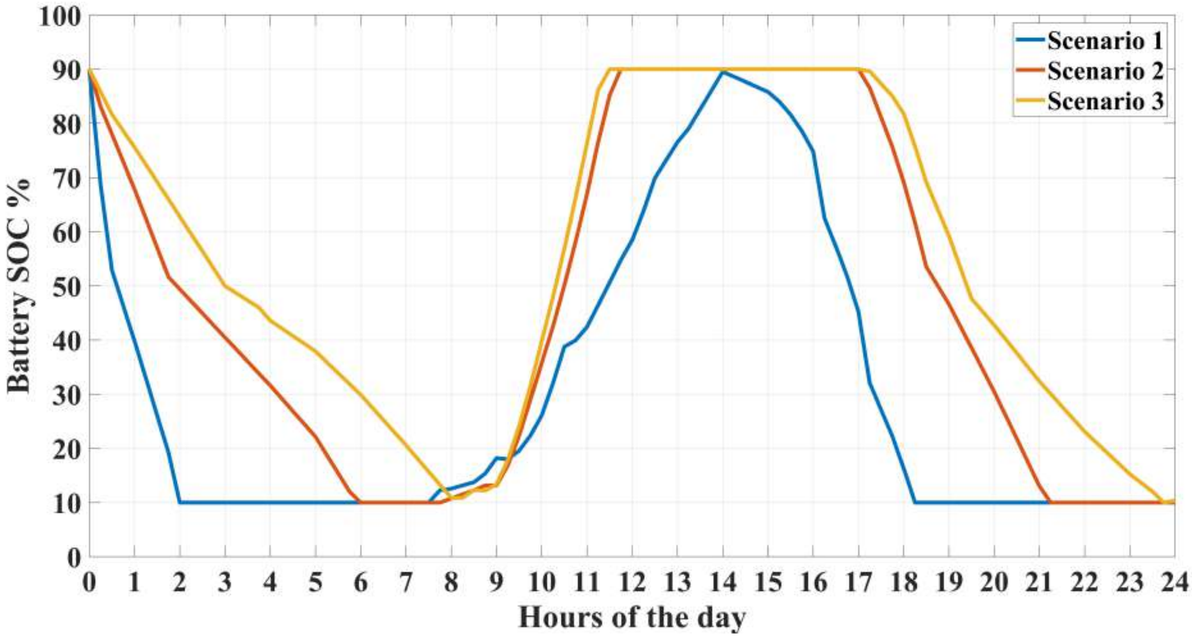

Figure 16: Battery SOC for the Hurricane Zeta

In Fig. 17, the battery SOC for all three scenarios is provided for Hurricane Ida. In scenario 1, the battery SOC stays at 10% for more than 9 hours, which is the maximum duration of hours in all the scenarios. In scenario 2, the battery SOC shows better characteristics, and SOC stays at 10% for around 5.5 hours. The SOC stays at 90% for around 2 hours, indicating that all the loads are served during that time. In scenario 3, the minimum SOC never reaches 10%, and the minimum SOC is 11.25%, which shows that at least priority load 1 is served for the whole 24 hours. The SOC remains 90% for around 3 hours, indicating that all the loads are served during that time.

In Fig. 18, the battery SOC for all three scenarios is provided for Hurricane Ida. In scenario 1, the battery SOC stays at 10% for around 13 hours, which is the maximum duration of hours in all the scenarios. After 1 hour from starting at 7 am, the SOC reaches a maximum of around 60%. In scenario 2, the battery SOC shows better characteristics, and SOC stays at 10% for around 10 hours. The SOC stays at 90% for around 3 hours, indicating that all the loads are served during that time. In scenario 3, the minimum SOC to reaches 10% for less than 7 hours, which shows the best performance among all the three scenarios. The SOC remains 90% for more than 4 hours, indicating that all the loads are served during that time.

4.3 Economic Assessment

Table 3 presents the investment required for 24 years considering scenarios 1, 2, and 3, respectively. Scenario 1 requires 147.95 thousand US dollars, whereas Scenario 2 requires 381.97 thousand dollars, which is more than 2.5 times the investment of Scenario 1.

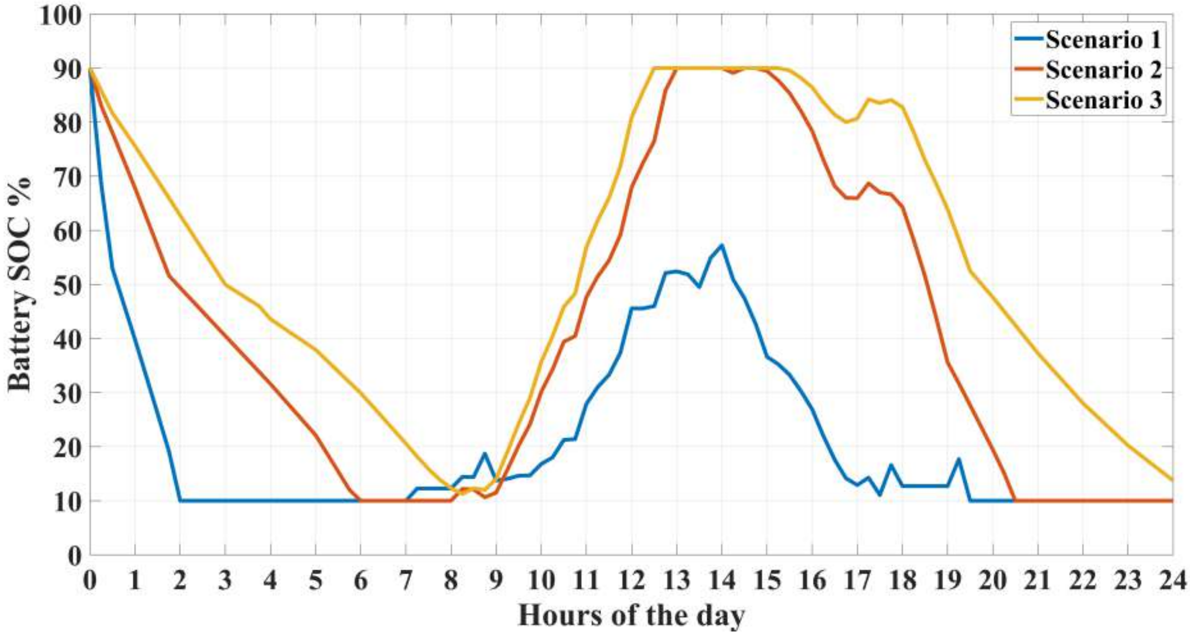

Figure 17: Battery SOC for the Hurricane Ida

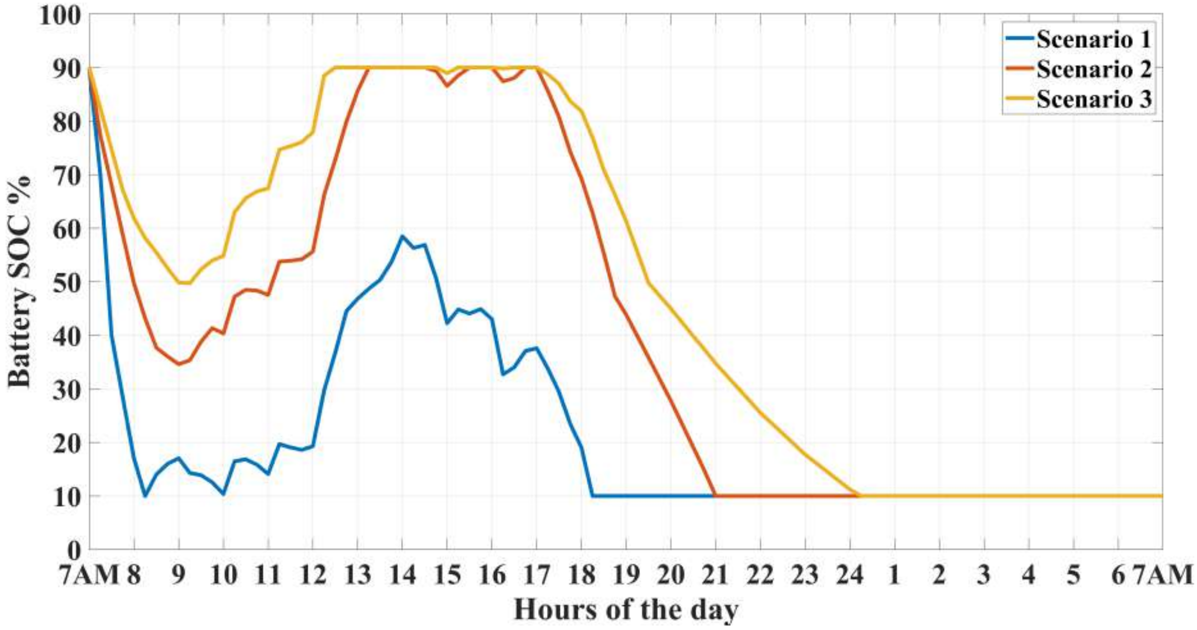

Figure 18: Battery SOC for the Hurricane Nate

Scenario 3 requires the maximum investment among all three scenarios, 739.75 thousand dollars.

Table 4 provides the profit produced during 24 years time duration for all three scenarios considering different numbers of hurricane sets. For one hurricane set (considering 4 hurricanes in 1 set) in 24 years, the profit of scenarios 1, 2, and 3 is 280.81, 716.29, and 769.29 thousand US dollars, respectively. For five hurricane sets (considering 4 hurricanes in 1 set) in 24 years, the profit of scenarios 1, 2, and 3 is 340.27, 844.45, and 946.85 thousand US dollars, respectively. It is visible that the monetary profit is increasing with the increasing number of hurricane sets for all three scenarios, and scenario 3 is the leading profit generator among all the hurricane sets.

Table 3: Investment for Three Scenarios (in thousands US $)

	Scenario 1	Scenario 2	Scenario 3
Investment	147.95	381.97	739.75

Table 4: Profit for Three Scenarios of Different Hurricane Sets (in thousands $)

Hurricane Sets	Scenario 1	Scenario 2	Scenario 3
1	280.81	716.29	769.29
2	293.16	742.91	806.17
3	307.05	772.86	847.66
4	322.68	806.55	894.34
5	340.27	844.45	946.85

For the in-depth analysis of the impacts of different numbers of hurricane sets in all three scenarios, three economic indicators, NPV, NPM, and RCR, are utilized for all three scenarios considering the number of hurricane sets from 1 to 5. In Fig. 19, NPV is increasing for all three scenarios with the increasing number of hurricane sets. Among all the hurricane sets, scenario 1 has the lowest NPV in all three scenarios. Although scenario 2 has the highest NPV for hurricane sets 1, 2, 3, and 4, scenario 3 achieves almost identical NPV of scenario 2 for hurricane sets 5. In Fig. 20, NPM curves portray the net profit margin for different hurricane sets. For all the different hurricane sets, NPM gradually increases for all three scenarios. Furthermore, scenario 1 is leading scenarios 2 and 3 for all the hurricane sets. Also, NPM curves for scenarios 1 and 2 are close which indicates that both scenarios are generating similar profits relative to their revenues. In Fig. 21, RCR graphs are presented for all three scenarios of different numbers of hurricane sets. For all the hurricane sets, all three scenarios have RCR value greater than 1, and the RCR value increases with the increasing number of hurricane sets.

5. Summary and conclusions

In conclusion, this manuscript introduces a pioneering Smart Investment Framework, empowering decision-makers to optimize energy resilience investments by aligning resources with desired resilience levels. Through a real-time simulation of a campus microgrid using Typhoon HIL, the study demonstrates the framework's practicality, showcasing the microgrid's effectiveness in powering local loads during outages. A quantitative analysis of resilience improvement costs adds economic depth to the framework, aiding decision-makers in balancing the economic burden with resilience goals. This research contributes

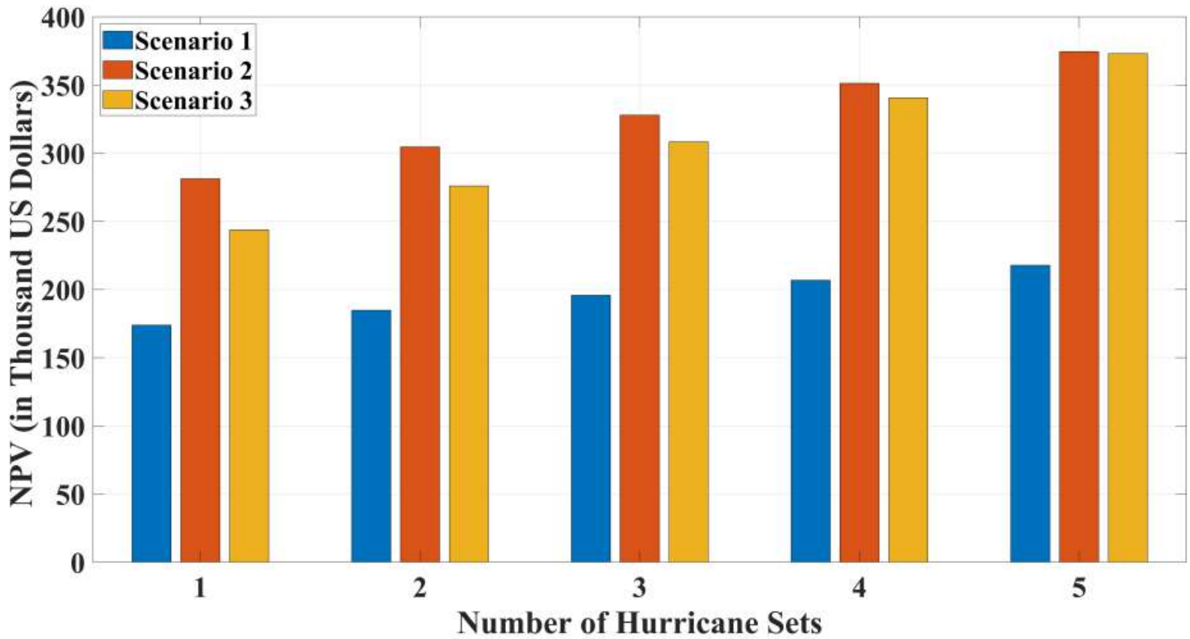

Figure 19: Net Present Value (NPV)

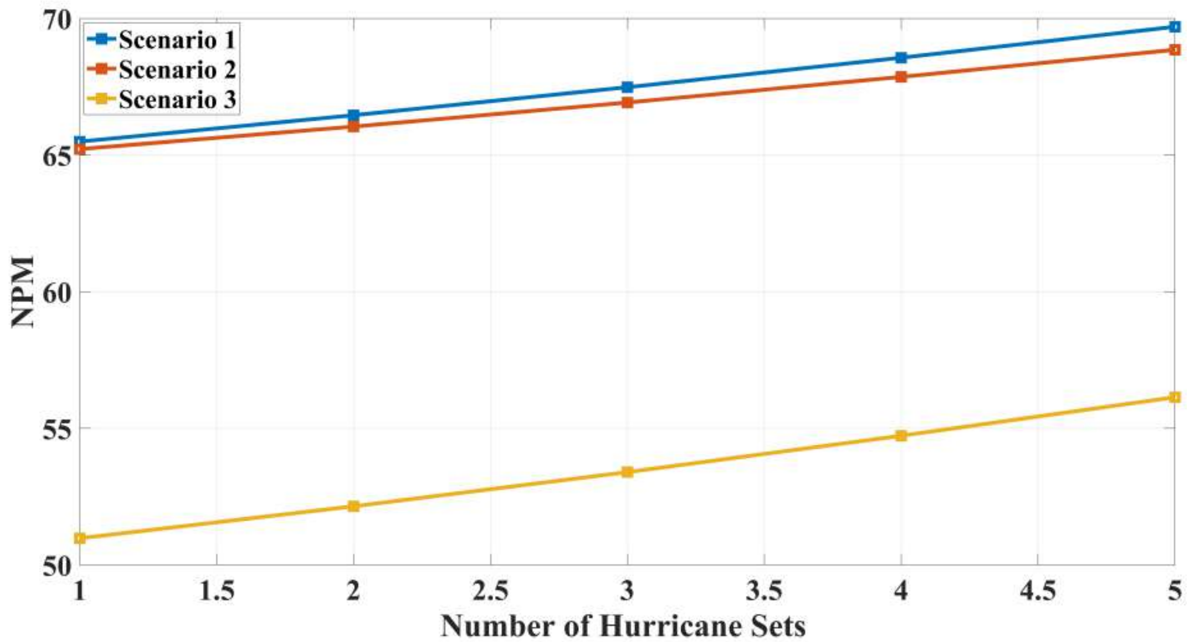

Figure 20: Net Profit Margin (NPM)

valuable insights for resilient energy infrastructure planning, offering a cost-effective approach to enhance resilience without unnecessary redundancy. The case study serves as a valuable guide for decision-makers in similar contexts, emphasizing the framework's potential in real-world applications.

6. What is Next

The current framework is entirely cost-driven. As a prospective avenue for further research, there is an opportunity to enhance the framework by integrating considerations

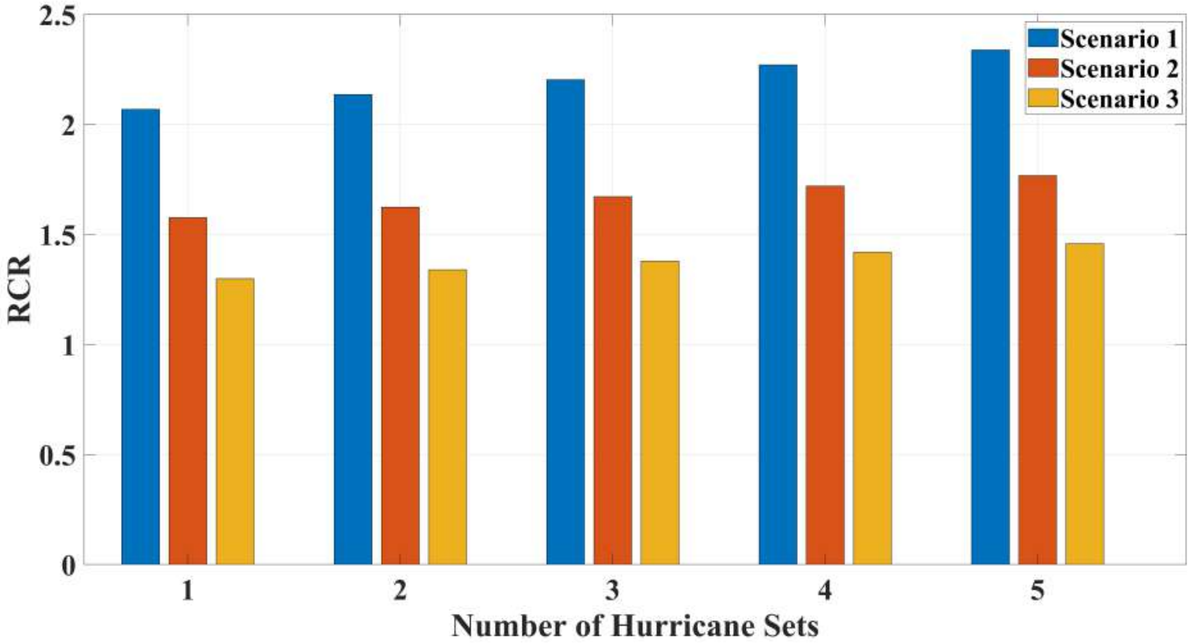

Figure 21: Revenue-Cost Ratio (RCR)

of energy equity. This exploration could involve evaluating how the proposed investment framework can be adapted to ensure fair and equitable distribution of energy resources, addressing social and economic disparities. This extension would contribute to a more comprehensive understanding of energy resilience, aligning with broader sustainability goals and promoting inclusivity in resilient energy infrastructure planning.

Acknowledgements

This research work is partially supported by the Louisiana Board of Regents, ITRS program as well as Cleco Power under the grant# LEQSF(2022-25)-RD-B-05

References

Abianeh, A. J., & Ferdowsi, F. (2020). Real time analysis of a multi-agent based distributed control strategy for islanded ac microgrids. *2020 clemson university power systems conference (PSC)*, 1–6.

Ali, M., Vasquez, J. C., Guerrero, J. M., Guan, Y., Golestan, S., De La Cruz, J., Koondhar, M. A., & Khan, B. (2023). A comparison of grid-connected local hospital loads with typical backup systems and renewable energy system based ad hoc microgrids for enhancing the resilience of the system. *Energies*, 16(4), 1918.

Anderson, K., Li, X., Dalvi, S., Ericson, S., Barrows, C., Murphy, C., & Hotchkiss, E. (2020). Integrating the value of electricity resilience in energy planning and operations decisions. *IEEE Systems Journal*, 15(1), 204–214.

Anusuya, K., Vijayakumar, K., & Manikandan, S. (2023). From efficiency to eternity: A holistic review of photovoltaic panel degradation and end-of-life management. *Solar Energy*, 265, 112135.

Arghandeh, R., Von Meier, A., Mehrmanesh, L., & Mili, L. (2016). On the definition of cyber-physical resilience in power systems. *Renewable and Sustainable Energy Reviews*, 58, 1060–1069.

Arora, P., & Ceferino, L. (2023). Probabilistic and machine learning methods for uncertainty quantification in power outage prediction due to extreme events. *Natural Hazards and Earth System Sciences*, 23(5), 1665–1683.

Benallal, A., Cheggaga, N., Ilinca, A., Tchoketch-Kebir, S., Ait Hammouda, C., & Barka, N. (2023). Bayesian inference-based energy management strategy for techno-economic optimization of a hybrid microgrid. *Energies*, 17(1), 114.

Bhusal, N., Abdelmalak, M., Kamruzzaman, M., & Benidris, M. (2020). Power system resilience: Current practices, challenges, and future directions. *IEEE Access*, 8, 18064–18086.

Bie, Z., Lin, Y., Li, G., & Li, F. (2017). Battling the extreme: A study on the power system resilience. *Proceedings of the IEEE*, 105(7), 1253–1266.

Choobineh, M., & Mohagheghi, S. (2015). Emergency electric service restoration in the aftermath of a natural disaster. *2015 IEEE Global Humanitarian Technology Conference (GHTC)*, 183–190.

Chowdhury, M. S., Rahman, K. S., Chowdhury, T., Nuthammachot, N., Techato, K., Akhtaruzzaman, M., Tiong, S. K., Sopian, K., & Amin, N. (2020). An overview of solar photovoltaic panels' end-of-life material recycling. *Energy Strategy Reviews*, 27, 100431.

Curtis, T., Heath, G., Walker, A., Desai, J., Settle, E., & Barbosa, C. (2021). *Best practices at the end of photovoltaic system performance period* (tech. rep.). National Renewable Energy Lab.(NREL), Golden, CO (United States).

Daeli, A., & Mohagheghi, S. (2023). Power grid infrastructural resilience against extreme events. *Energies*, 16(1), 64.

Das, L., Munikoti, S., Natarajan, B., & Srinivasan, B. (2020). Measuring smart grid resilience: Methods, challenges and opportunities. *Renewable and Sustainable Energy Reviews*, 130, 109918.

Deotti, L., Guedes, W., Dias, B., & Soares, T. (2020). Technical and economic analysis of battery storage for residential solar photovoltaic systems in the brazilian regulatory context. *Energies*, 13(24), 6517.

Ding, T., Wang, Z., Jia, W., Chen, B., Chen, C., & Shahidehpour, M. (2020). Multiperiod distribution system restoration with routing repair crews, mobile electric vehicles, and soft-open-point networked microgrids. *IEEE Transactions on Smart Grid*, 11(6), 4795–4808.

Dugan, J., Mohagheghi, S., & Kroposki, B. (2021). Application of mobile energy storage for enhancing power grid resilience: A review. *Energies*, 14(20), 6476.

Ferdowsi, F., Dabbaghjamanesh, M., Mehraeen, S., & Rastegar, M. (2019). Optimal scheduling of reconfigurable hybrid ac/dc microgrid under dlr security constraint. *2019 IEEE Green Technologies Conference (GreenTech)*, 1–5.

Force, I. P. T., Stanković, A., Tomsovic, K., De Caro, F., Braun, M., Chow, J., Äukalevski, N., Dobson, I., Eto, J., Fink, B., et al. (2022). Methods for analysis and quantification of power system resilience. *IEEE Transactions on Power Systems*.

Gandhi, O., Rodríguez-Gallegos, C. D., Gorla, N. B. Y., Bieri, M., Reindl, T., & Srinivasan, D. (2018). Reactive power cost from pv inverters considering inverter lifetime assessment. *IEEE Transactions on Sustainable Energy*, 10(2), 738–747.

Gao, H., Chen, Y., Mei, S., Huang, S., & Xu, Y. (2017). Resilience-oriented pre-hurricane resource allocation in distribution systems considering electric buses. *Proceedings of the IEEE*, 105(7), 1214–1233.

Gholami, A., Shekari, T., Aminifar, F., & Shahidehpour, M. (2016). Microgrid scheduling with uncertainty: The quest for resilience. *IEEE Transactions on Smart Grid*, 7(6), 2849–2858.

Hamidieh, M., & Ghassemi, M. (2022). Microgrids and resilience: A review. *IEEE Access*.

Hoke, A., Butler, R., Hambrick, J., & Kroposki, B. (2012). Steady-state analysis of maximum photovoltaic penetration levels on typical distribution feeders. *IEEE Transactions on Sustainable Energy*, 4(2), 350–357.

Hossain, E., Roy, S., Mohammad, N., Nawar, N., & Dipta, D. R. (2021). Metrics and enhancement strategies for grid resilience and reliability during natural disasters. *Applied energy*, 290, 116709.

Humphreys, K., & Brown, D. (1990). *Life-cycle cost comparisons of advanced storage batteries and fuel cells for utility, stand-alone, and electric vehicle applications* (tech. rep.). Pacific Northwest Lab., Richland, WA (USA).

Igder, M. A., Liang, X., & Mitolo, M. (2022). Service restoration through microgrid formation in distribution networks: A review. *IEEE Access*, 10, 46618–46632.

Janić, M. (2018). Modelling the resilience of rail passenger transport networks affected by large-scale disruptive events: The case of hsr (high speed rail). *Transportation*, 45, 1101–1137.

Kenward, A., Raja, U., et al. (2014). Blackout: Extreme weather, climate change and power outages. *Climate central*, 10, 1–23.

Khodayar, M. E., Barati, M., & Shahidehpour, M. (2012). Integration of high reliability distribution system in microgrid operation. *IEEE Transactions on Smart Grid*, 3(4), 1997–2006. https://doi.org/10.1109/TSG.2012.2213348

Lei, S., Chen, C., Zhou, H., & Hou, Y. (2018). Routing and scheduling of mobile power sources for distribution system resilience enhancement. *IEEE Transactions on Smart Grid*, 10(5), 5650–5662.

Lei, S., Wang, J., Chen, C., & Hou, Y. (2016). Mobile emergency generator pre-positioning and real-time allocation for resilient response to natural disasters. *IEEE Transactions on Smart Grid*, 9(3), 2030–2041.

Li, Z., Shahidehpour, M., Aminifar, F., Alabdulwahab, A., & Al-Turki, Y. (2017). Networked microgrids for enhancing the power system resilience. *Proceedings of the IEEE*, 105(7), 1289–1310.

Lin, Y., Wang, J., & Yue, M. (2022). Equity-based grid resilience: How do we get there? *The Electricity Journal*, 35(5), 107135.

Liu, G., Ollis, T. B., Zhang, Y., Jiang, T., & Tomsovic, K. (2020). Robust microgrid scheduling with resiliency considerations. *IEEE Access*, 8, 153169–153182.

Lund, P. D. (2018). Capacity matching of storage to pv in a global frame with different loads profiles. *Journal of Energy Storage*, 18, 218–228.

Mishra, S., Anderson, K., Miller, B., Boyer, K., & Warren, A. (2020). Microgrid resilience: A holistic approach for assessing threats, identifying vulnerabilities, and designing corresponding mitigation strategies. *Applied Energy*, 264, 114726.

Moglen, R. L., Barth, J., Gupta, S., Kawai, E., Klise, K., & Leibowicz, B. D. (2023). A nexus approach to infrastructure resilience planning under uncertainty. *Reliability Engineering & System Safety*, 230, 108931.

Mohammadian, M., Aminifar, F., Amjady, N., & Shahidehpour, M. (2021). Data-driven classifier for extreme outage prediction based on bayes decision theory. *IEEE Transactions on Power Systems*, 36(6), 4906–4914.

Mongird, K., Viswanathan, V., Balducci, P., Alam, J., Fotedar, V., Koritarov, V., & Hadjerioua, B. (2020). An evaluation of energy storage cost and performance characteristics. *Energies*, 13(13), 3307.

Mukhopadhyay, S., & Nateghi, R. (2017). Estimating climate—demand nexus to support longterm adequacy planning in the energy sector. *2017 IEEE Power & Energy Society General Meeting*, 1–5.

Nazemi, M., Dehghanian, P., Lu, X., & Chen, C. (2021). Uncertainty-aware deployment of mobile energy storage systems for distribution grid resilience. *IEEE Transactions on Smart Grid*, 12(4), 3200–3214.

Noaa national centers for environmental information (ncei). (2022).

of the President. Council of Economic Advisers, E. O. (2013). *Economic benefits of increasing electric grid resilience to weather outages*. The Council.

Panteli, M., Mancarella, P., Trakas, D. N., Kyriakides, E., & Hatziargyriou, N. D. (2017). Metrics and quantification of operational and infrastructure resilience in power systems. *IEEE Transactions on Power Systems*, 32(6), 4732–4742.

Ramasamy, V., Zuboy, J., O'Shaughnessy, E., Feldman, D., Desai, J., Woodhouse, M., Basore, P., & Margolis, R. (2022). *Us solar photovoltaic system and energy storage cost benchmarks, with minimum sustainable price analysis: Q1 2022* (tech. rep.). National Renewable Energy Lab.(NREL), Golden, CO (United States).

Raoufi, H., Vahidinasab, V., & Mehran, K. (2020). Power systems resilience metrics: A comprehensive review of challenges and outlook. *Sustainability*, 12(22), 9698.

Schweikert, A. E., & Deinert, M. R. (2021). Vulnerability and resilience of power systems infrastructure to natural hazards and climate change. *Wiley Interdisciplinary Reviews: Climate Change*, 12(5), e724.

Sedzro, K. S. A., Shi, X., Lamadrid, A. J., & Zuluaga, L. F. (2018). A heuristic approach to the post-disturbance and stochastic pre-disturbance microgrid formation problem. *IEEE Transactions on Smart Grid*, 10(5), 5574–5586.

Tan, V., Dias, P. R., Chang, N., & Deng, R. (2022). Estimating the lifetime of solar photovoltaic modules in australia. *Sustainability*, 14(9), 5336.

Ullah, S. S., Abianeh, A. J., Osunwoke, E. B., & Ferdowsi, F. (2021). Comparative analysis of volt-var control parameter settings of smart pv inverters: A case study. *2021 North American Power Symposium (NAPS)*, 01–06.

Ullah, S. S., Ebrahimi, S., Ferdowsi, F., & Barati, M. (2023). Techno-economic impacts of volt-var control on the high penetration of solar pv interconnection. *Cleaner Energy Systems*, 100067.

Veerendra Kumar, D. J., Deville, L., Ritter III, K. A., Raush, J. R., Ferdowsi, F., Gottumukkala, R., & Chambers, T. L. (2022). Performance evaluation of 1.1 mw grid-connected solar photovoltaic power plant in louisiana. *Energies*, 15(9), 3420.

Vugrin, E. D., Castillo, A. R., & Silva-Monroy, C. A. (2017). *Resilience metrics for the electric power system: A performance-based approach.* (tech. rep.). Sandia National Lab.(SNL-NM), Albuquerque, NM (United States).

Yao, S., Gu, J., Zhang, H., Wang, P., Liu, X., & Zhao, T. (2020). Resilient load restoration in microgrids considering mobile energy storage fleets: A deep reinforcement learning approach. *2020 IEEE Power & Energy Society General Meeting (PESGM)*, 1–5.

Yao, S., Wang, P., Liu, X., Zhang, H., & Zhao, T. (2019). Rolling optimization of mobile energy storage fleets for resilient service restoration. *IEEE Transactions on Smart Grid*, 11(2), 1030–1043.

Yao, S., Wang, P., & Zhao, T. (2018). Transportable energy storage for more resilient distribution systems with multiple microgrids. *IEEE Transactions on Smart Grid*, 10(3), 3331–3341.

Yao, S., Zhao, T., Zhang, H., Wang, P., & Goel, L. (2018). Two-stage stochastic scheduling of transportable energy storage systems for resilient distribution systems. *2018 IEEE International Conference on Probabilistic Methods Applied to Power Systems (PMAPS)*, 1–6.